AFML-TR-67-289

CYCLIC HOT-SALT STRESS CORROSION OF TITANIUM ALLOYS

L. H. Stone
A. H. Freedman
Northrop Corporation

TECHNICAL REPORT AFML-TR-67-289

September 1967

Air Force Materials Laboratory
Research and Technology Division
Air Force Systems Command
Wright-Patterson Air Force Base, Ohio

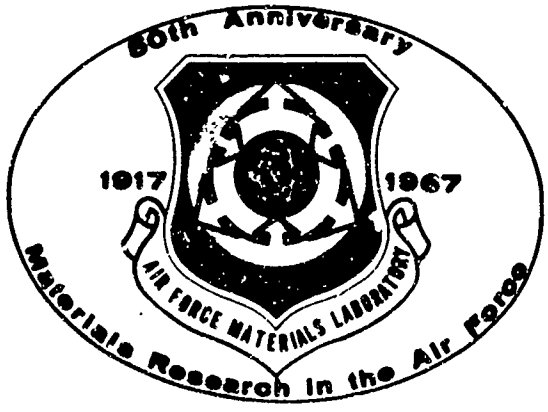

NOTICE

When Government drawings, specifications, or other data are used for any purpose other than in connection with a definitely related Government procurement operation, the United States Government thereby incurs no responsibility nor any obligation whatsoever; and the fact that the Government may have formulated, furnished, or in any way supplied the said drawings, specifications, or other data, is not to be regarded by implication or otherwise as in any manner licensing the holder or any other person or corporation, or conveying any rights or permission to manufacture, use, or sell any patented invention that may in any way be related thereto.

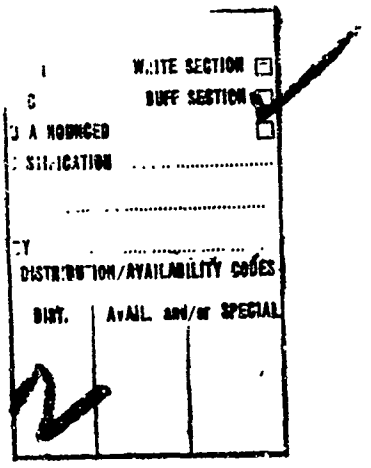

Copies of this report should not be returned unless return is required by security considerations, contractual obligations, or notice on a specific document.

CYCLIC HOT-SALT STRESS CORROSION OF TITANIUM ALLOYS

L. H. Stone
A. H. Freedman

FOREWORD

This report was prepared by the Materials Research Group of Northrop Norair, a Division of Northrop Corporation, under USAF Contract No. AF 33 (615)-3642. The contract work was performed under Project No. 7381, "Materials Application", and Task No. 738107 "Detection, Control, and Prevention of Corrosion". The research activities discussed in this Technical Report cover the period from 1 March 1966 through 30 May 1967. This report was submitted for publication 18 December 1967. Report No. NOR 67-151 has been assigned for internal control.

The work was administered under the direction of the Air Force Materials Laboratory, Research and Technology Division, with Mr. George M. Yoder, MAAE, serving as project engineer.

The program at Northrop Norair was performed with Mr. L. H. Stone serving as project experimentalist and Mr. A. H. Freedman serving as principal investigator.

Additional Northrop Norair personnel who made major contributions to the effort described in this report were: Messrs. H. R. Miller, R. E. Herfert, H. E. Longman, J. Abger, and R. E. Rosas.

This Technical Report has been reviewed and is approved.

W. P. Conrardy

W. P. CONRARDY, Chief
Systems Support Branch
Materials Applications Division
Air Force Materials Laboratory

ABSTRACT

Hot-salt stress-corrosion cracking of Ti-6Al-4V, Ti-8Al-1Mo-1V, Ti-13V-11Cr-3Al, Ti-6Al-6V-2Sn, and Ti-679 was investigated for both continuous exposure and a specified, cyclic, thermal exposure representing a typical Mach 3 mission. The effects of heat treatment and material thickness were also studied.

Initial tests on fatigue-cracked specimens showed that hot-salt stress-corrosion cracking is not controlled by fracture mechanics because new surface cracks nucleate and grow in preference to an existing fatigue crack. Therefore, all subsequent tests were conducted on smooth specimens.

At 450F, only mill-annealed Ti-8Al-1Mo-1V showed stress-corrosion cracking. At 550F and 650F, individual threshold values of stress were established for each material below which no cracking occurred for either continuous or cyclic exposure. Most of these threshold levels lay between 0.35 and 0.50 of the yield strength at 550F and between 0.25 and 0.45 of the yield strength at 650F.

At stress levels just above threshold values, cyclic nucleation times were substantially longer than continuous nucleation times. As the stress level increased, this difference decreased, and at high stress levels, both nucleation times were essentially the same. Welding produced no detrimental effects on the stress corrosion behavior of Ti-8Al-1Mo-1V and Ti-6Al-4V. Welded specimens had much longer nucleation times, cyclic or continuous, than the parent metal at 550F; at 650F, the continuous nucleation times for welded specimens approximated those for the parent materials, but the cyclic nucleation times were substantially longer. The behavior of welded specimens may have been influenced by the presence of compressive surface residual stresses produced during specimen preparation.

The kinetics of the formation of $TiCl_2$ on NaCl-coated titanium alloys and of its decomposition at room temperature were measured by X-ray diffraction. Detectable amounts of $TiCl_2$ appeared after periods of 0.25 to 17 hours for various alloys at temperatures from 550F to 730F. Decomposition times at room temperature were relatively constant at 4 to 5 hours. Specimens were subjected to a special cycle of heating at 550F for less time than that to produce detectable $TiCl_2$ and holding at room temperature for longer than needed to decompose $TiCl_2$. These specimens did not show cracking in times well beyond the nucleation times for the standard cycle.

The results of this program indicate a strong possibility for eliminating hot-salt stress corrosion of titanium structures operating above 550F, even at high stresses, if the thermal cycles to which the structure is exposed can be controlled. The time at temperature should be less than the time to form $TiCl_2$, and the time between cycles at room temperature greater than the time required to decompose $TiCl_2$.

TABLE OF CONTENTS

LIST OF ILLUSTRATIONS

LIST OF TABLES

I INTRODUCTION

Laboratory tests have established that titanium alloys are susceptible to hot-salt stress-corrosion cracking at elevated temperatures. In contrast, stress-corrosion cracking has not been found in titanium parts operating in aircraft at elevated temperatures in a marine atmosphere. However, the majority of laboratory tests have been based upon continuous elevated-temperature exposures, whereas service experience has involved short-time cyclic exposures at elevated temperatures. Limited laboratory data[1] have shown that hot-salt stress corrosion is reduced significantly by thermal cycling.

A plausible explanation for this anomaly is that hot-salt stress corrosion of titanium alloys requires a nucleation time at elevated temperature to establish the chemical cell necessary for initiation of stress-corrosion cracking. Each time the temperature is reduced, the equilibrium chemical cell may be changed in a manner to retard or stop the stress-corrosion process. Upon reheating to an elevated temperature, time may be required to renucleate the stress-corrosion chemical cell before cracking is possible. If typical flight profiles involve thermal exposure times less than the nucleation time, stress-corrosion cracking may be suppressed.

The purpose of this investigation has been to determine nucleation times for hot-salt (NaCl) stress corrosion as a function of stress and temperature for several titanium alloys under continuous and cyclic thermal exposures. This information will establish:

1. Whether thermal conditions in real flight are close to a critical time of nucleation.

2. Whether repeated thermal exposures below a nucleation time are independent or cumulative to some degree with respect to stress-corrosion cracking.

Single-edge-notched and fatigue-cracked specimens, modified NASA self-stressed specimens, and smooth tensile specimens were selected for determination of stress-corrosion nucleation times under cyclic and continuous thermal exposures.

II MATERIALS

Titanium alloys included in this program are Ti-6Al-4V (Ti64), Ti-8Al-1Mo-1V (Ti811), and Ti-13V-11Cr-3Al (B120) in the form of 0.030 - 0.040 inch sheet and 1/8-inch plate, and Ti-6Al-6V-2Sn (Ti662) and Ti-2.5Al-11.5Sn-6Zr-1.2Mo-0.27Si (Ti679) in the form of 1/8-inch plate. Weldments of 1/8-inch Ti811DA (duplex annealed) and Ti64STA (solution treated and aged) were also included. The alloys were procured from Titanium Metals Corporation of America with the as-received heat treatments and chemical analyses shown in Table I.

TABLE I

CHEMICAL ANALYSES OF TITANIUM ALLOYS

ALLOY	NOMINAL GAGE (inch)	HEAT NUMBER	AS-RECEIVED HEAT TREATMENT	INGOT CHEMICAL ANALYSES (weight percent)
Ti-8Al-1Mo-1V	.035	G-676	8 Hrs. at 1450F, Furnace Cool + 15 Min. at 1450F, Air Cool (Duplex Annealed)	C-.023, Fe-.05, N-.013, Al-7.8, V-1.0, Mo-1.0. H-.005-.009, O_2-.08
Ti-8Al-1Mo-1V	.125	D-8733	Same as Sheet	C-.023, Fe-.08, N-.011, Al-7.8, V-1.0, Mo-1.1, H-.005, O_2-.10
Ti-6Al-4V	.040	G-786	1 Min. at 1670F, Water Quench + 4 Hrs. at 1000F, Air Cool (Solution Treated and Aged)	C-.023, Fe-.11, N-.008, Al-5.9, V-4.0, H-.011-.013, O_2-.14
Ti-6Al-4V	.125	D-9701	3 Min. at 1670F, Water Quench + 4 Hrs. at 1000F, Air Cool (Solution Treated and Aged)	C-.023, Fe-.09, N-.012, Al-5.9, V-4.0, H-.008, O_2-.11
Ti-13V-11Cr-3Al	.040	D-8053	15 Min. at 1450F, Air Cool (Solution Treated)	C-.025, Fe-.15, N-.026, Al-3.1, V-13.5, Cr-11.0, H-.012, O_2-.13
Ti-13V-11Cr-3Al	.125	I-8988	Same as Sheet	C-.014, Fe-.17, N-.015, Al-3.0, V-13.7, Cr-10.6, H-.007, O_2-.15
Ti-6Al-6V-2Sn	.120	G-71	15 Min. at 1350F, Furnace Cool (Annealed)	C-.026, Fe-.66, N-.014, Al-5.5, V-5.5, Sn-1.8, Mn-.65, H-.006, O_2-.17
Ti-679	.125	D-7274	30 Min. at 1650F, Air Cool + 24 Hrs. at 900F, Air Cool (Solution Treated and Aged)	C-.023, Fe-.08, N-.012, Al-2.4, Mo-.97, Zr-4.7, Sn-10.8, Si-.23, H-.005-.006

III PROCEDURES

MECHANICAL PROPERTIES

Transverse tensile properties of the alloys were determined at 450F, 550F, and 650F to qualify the program materials and heat treatments. Several tensile coupons of each alloy were tested in the as-received condition or heat treated according to the schedule shown in Table II. Tensile coupons of Ti811, Ti64, and B120 were annealed in a cold-wall vacuum furnace. Solution-treated tensile specimens of B120 were encapsulated in an evacuated envelope of stainless steel and aged in a recirculating air furnace.

The Ti662 tensile coupons were solution treated in an air furnace and water quenched. Surface contamination was removed by alternately etching in a $5HF-35HNO_3-60H_2O$ solution operating at room temperature and brushing to remove corrosion products. A total etching time of 30 minutes was employed to remove 0.002 inch per side. Subsequent aging of these specimens was performed in the cold-wall vacuum furnace.

Because the Ti679 was received sheared to 6-inch lengths, the 1/2-inch wide tensile specimens made from it had only 1-inch gage lengths. Other alloys were tested using standard specimens of 2-inch gage length and 1/2-inch width.

EDGE-NOTCHED SPECIMENS

Figure 1 shows the single-edge-notched and fatigue-cracked specimens of sheet and plate which were employed to study stress-corrosion nucleation times in the presence of a crack. Each specimen was scrubbed with cleanser and alkaline cleaned prior to tension-tension fatigue cracking at a net section stress of approximately 20,000 psi maximum and 2000 psi minimum using a 3600 cpm fatigue machine.

Salt was placed in the fatigue cracks as discussed in a subsequent section of this report. In some cases, the specimen surfaces were also coated with 0.002 ± 0.0005 inch of NaCl applied by heating the specimens to 400-450F followed by spraying a hot aqueous solution of NaCl.

Specimens were dead-weight loaded in a lever-arm fixture and heated by quartz lamps. A transit was used to measure crack growth during a test. After testing, specimens were fractured and examined visually and by electron microscope fractography. The nucleation time for stress corrosion was defined as the time required to produce 0.004 - 0.010 inch of crack growth by stress corrosion.

SELF-STRESSED SPECIMENS

Modified NASA self-stressed sheet specimens were fabricated from 4 x 0.350 x 0.035 - 0.040 inch strips to provide a width-to-thickness ratio of approximately 10 and a biaxiality ratio of 0.50[2]. The standard NASA specimen of 1/4-inch width provided a width-to-thickness ratio of 6.25 and a biaxiality ratio of 0.45 using 0.040-inch-thick material.

TABLE II

HEAT TREATMENT SCHEDULE FOR TITANIUM ALLOYS

ALLOY	CONFIGURATION	AS-RECEIVED HEAT TREATMENT	REQUIRED HEAT TREATMENTS	ADDITIONAL HEAT TREATMENT (1)
Ti-6Al-4V	Sheet and Plate	Solution Treated and Aged	1) Solution Treated & Aged 2) Annealed	1) Anneal: 4 Hrs. at 1350F, Furnace Cool
Ti-8Al-1Mo-1V	Sheet and Plate	Duplex Annealed	1) Duplex Annealed 2) Mill Annealed	1) Mill Anneal: 8 Hrs. at 1450F, Furnace Cool
Ti-13V-11Cr-3Al	Sheet and Plate	Solution Treated	1) Solution Treated & Aged 2) Annealed	1) Age: 24 Hrs. at 900F, Air Cool 2) Anneal: 30 Min. at 1425F, Furnace Cool
Ti-6Al-6V-2Sn	Plate	Annealed	1) Solution Treated & Aged 2) Annealed	1) Solution Treat and Age: 5 Min. at 1550F, Water Quench + 4 Hrs. at 1100F, Furnace Cool
Ti-679	Plate	Solution Treated and Aged	1) Solution Treated & Aged	None

HEAT-TREATMENT DESIGNATIONS

STA - Solution Treated and Aged
A - Annealed
DA - Duplex Annealed
MA - Mill Annealed

(1) Performed at Norair

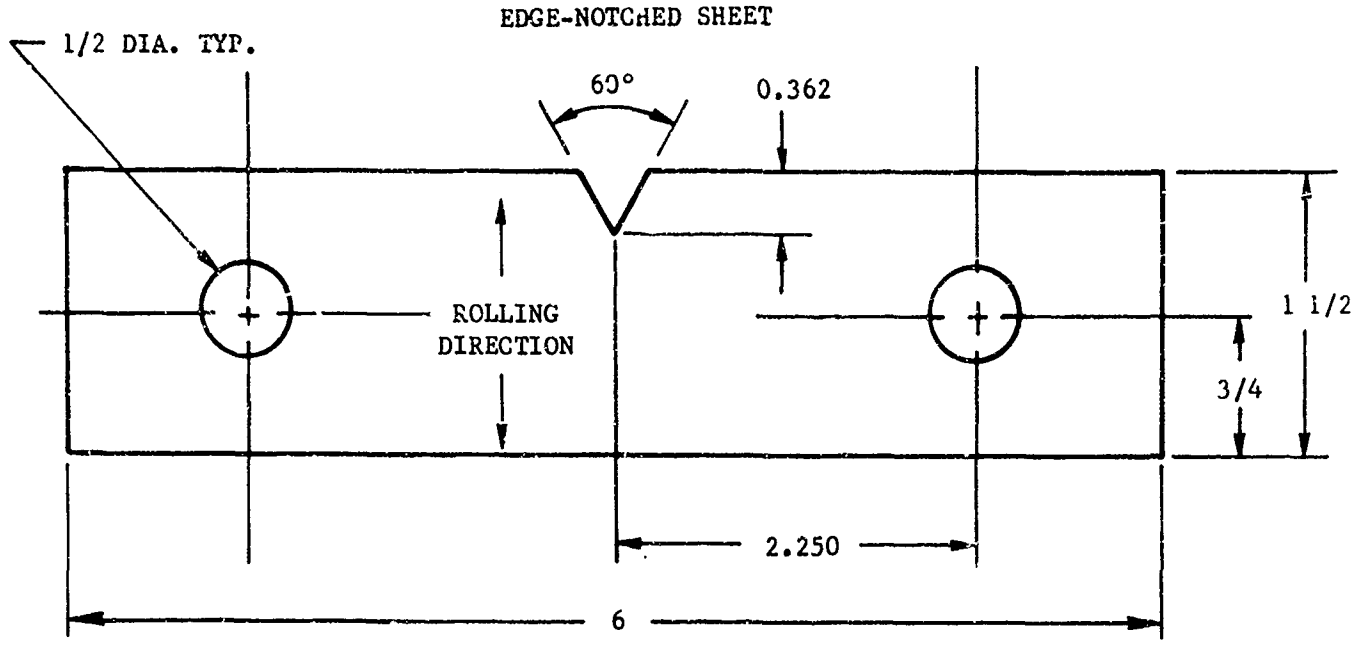

FATIGUE CRACK LENGTH - 2.5t
(0.100 ± 0.010 INCH) FROM NOTCH ROOT

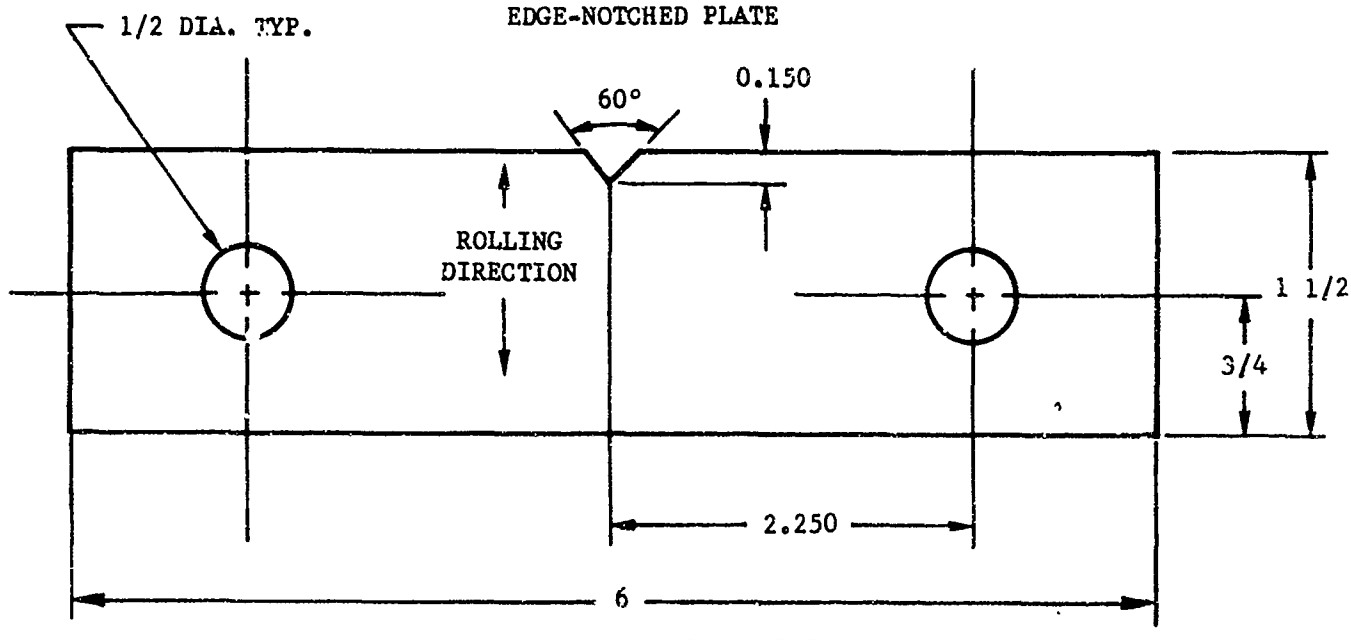

FATIGUE CRACK LENGTH - 2.5t
(0.312 ± 0.010 INCH) FROM NOTCH ROOT

FIGURE 1 SINGLE-EDGE-NOTCHED SHEET AND PLATE SPECIMENS

Specimen blanks were sheared with the width parallel to the rolling direction and machined to size. The ends were bent to the desired angle, and the strips were alkaline cleaned, etched in a $2HF\text{-}25HNO_3\text{-}73H_2O$ solution, and spot welded together to produce the configuration shown in Figure 2. The bend angle required to produce a given stress was determined by trial and error. The separation distance, d, (Figure 2) required to produce a given stress was determined from the following relationship[3]:

$$d = \frac{tE}{\sigma} - \left(\frac{t^2E^2}{\sigma^2} - C^2\right)^{1/2}$$

where

t = sheet thickness - inch

E = Young's modulus at test temperature - psi

σ = maximum fiber stress - psi

C = 2.5 inches.

The center regions of each specimen were coated with 0.002 ± 0.0005 inch of salt on the tension sides using the hot spray technique. After thermal exposure, salt and corrosion products were removed by scrubbing with cleanser followed by swab etching in $2HF\text{-}25HNO_3\text{-}73H_2O$; visual examination at 500X was employed to detect stress-corrosion crack formation.

SMOOTH TENSILE SPECIMENS

Smooth tensile specimens were fabricated to the configuration shown in Figure 3. Since thickness varied somewhat among the sheet and plate materials, specimen widths were adjusted to provide specimens of constant cross-sectional area.

Procedures for cleaning, salt coating, removal of salt and corrosion products, and examination for cracking followed those for self-stressed specimens. Testing was conducted under dead-weight lever-arm loading and quartz-lamp heating as employed for the fatigue-cracked specimens.

WELDED SPECIMENS

Several Ti64STA (solution treated and aged) and Ti811DA (duplex annealed) plates 3 x 15 x 1/8 inch were welded by the automatic TIG process using the welding parameters shown in Table III. A double bevel was used for joints welded with commercially pure titanium (Ti-75A) filler to minimize base alloy dilution. The weld bead was milled flush with the base alloy and approximately .002 inch was also removed simultaneously from the heat-affected zone and adjacent base alloy. Each weldment was X-rayed before smooth tensile specimens were machined to configuration shown in Figure 3. The fusion zone of each specimen was on the specimen centerline perpendicular to the loading direction and parallel to the rolling direction. Machined surfaces were hand-sanded to provide a smooth surface for examination after stress-corrosion testing. Cleaning, salt coating, and testing procedures were the same as the procedures used for smooth tensile specimens of the parent materials.

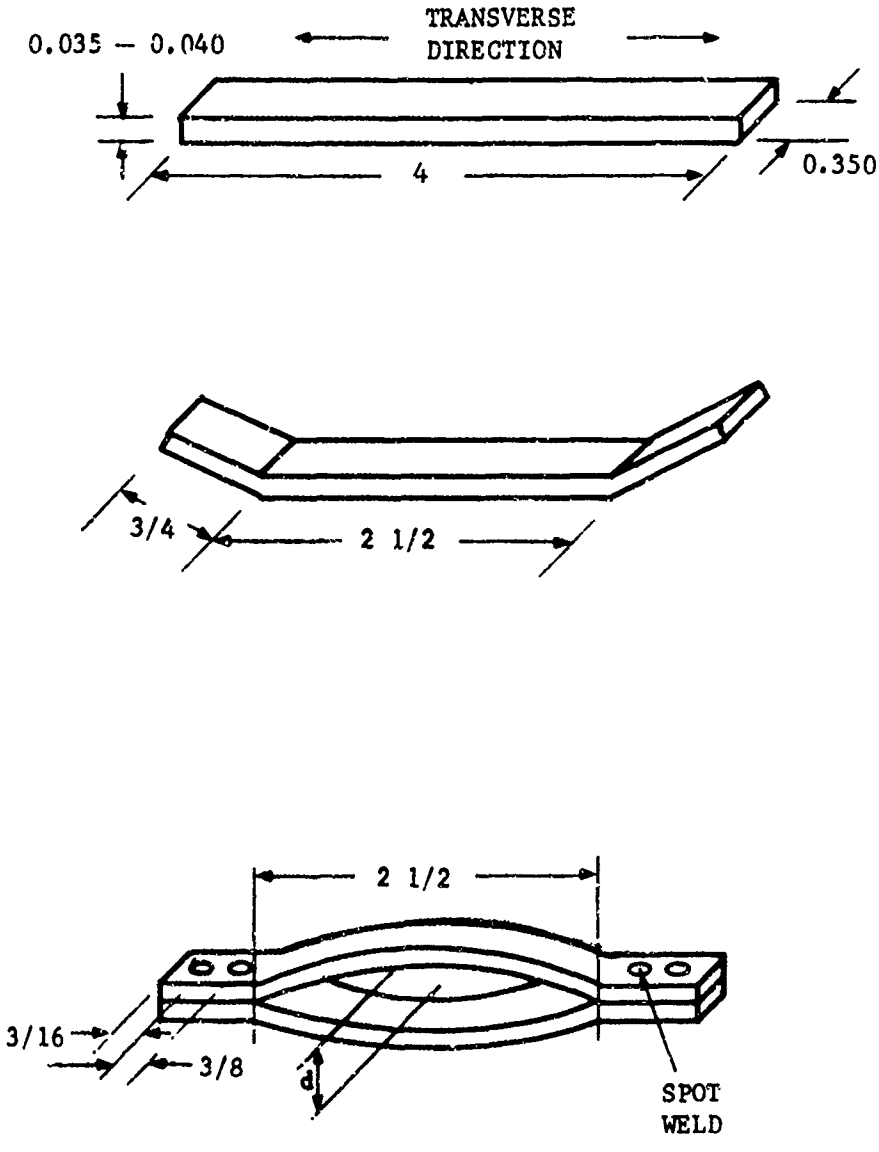

FIGURE 2 MODIFIED NASA SELF-STRESSED SPECIMEN

TABLE III

AUTOMATIC TIG WELDING PARAMETERS

BASE ALLOY	HEAD TRAVEL (inch per min.)	CURRENT (amps)	VOLTAGE	GAS FLOW (cfh)			ELECTRODE		HOLD DOWN		FILLER WIRE		BACKUP MATERIAL	PRE-HEAT	PASS
				TORCH	TRAILING	BACKUP	DIAMETER (inch)	GEOMETRY (inch)	SPACING (inch)	PRESSURE (pounds)	TYPE	DIAMETER (inch)			
T164STA(1)	6	120	8	20	60+	20	1/8	3/4 Taper .030 Ball	7/8	120	None	-	Stainless Steel	None	1st
		160									T164	.045			2nd
T164STA(2)		130									None	-			1st
		130									T175A	.045			2nd
T1811DA(1)		120									None	-			1st
		160									T1811	.062			2nd
T1811DA(2)		130									None	-			1st
		130									T175A	.045			2nd

NOTES: (1) Singlo V bevel

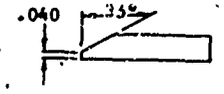

(2) Double V bevel

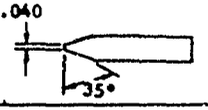

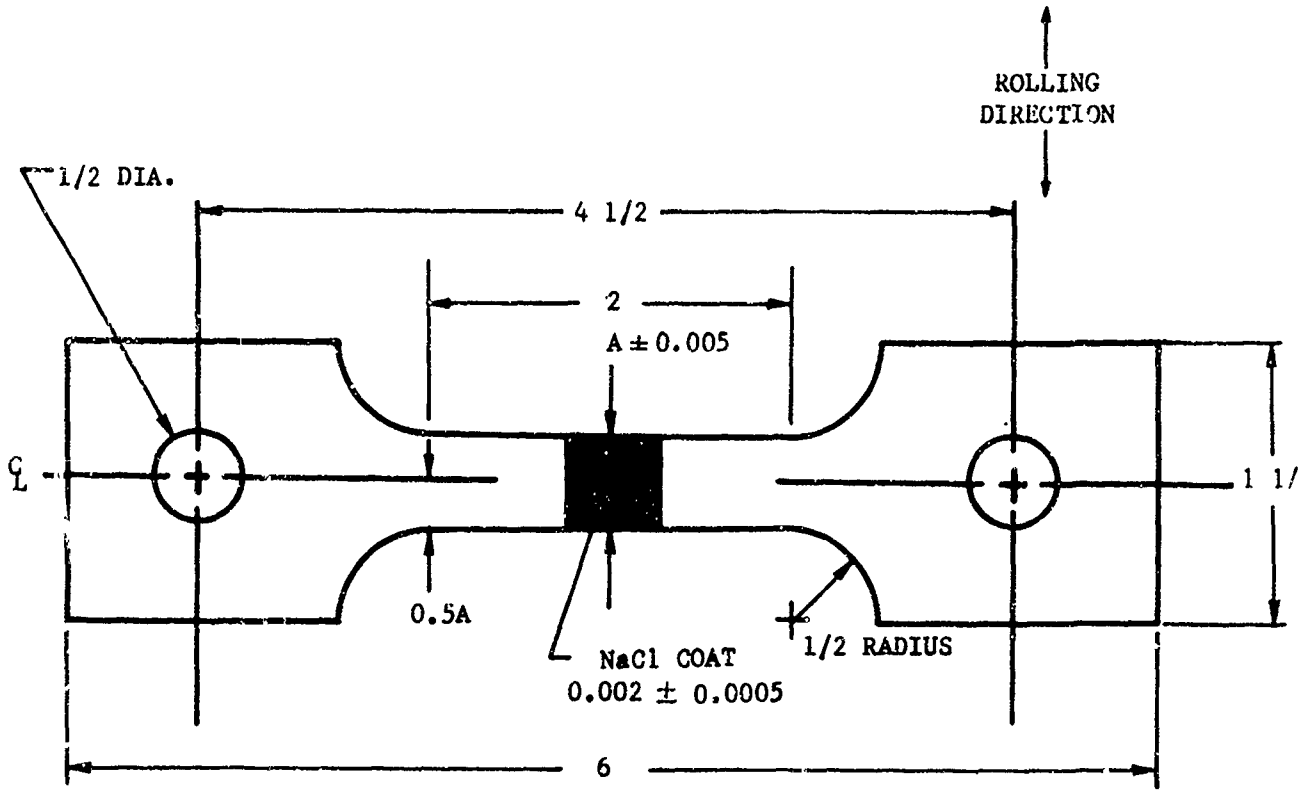

ALL DIMENSIONS IN INCHES

ALLOY	THICKNESS	"A" DIMENSION
Ti-8Al-1Mo-1V	0.035 Inch	0.557 Inch
Ti-8Al-1Mo-1V	0.125	0.500
Ti-6Al-4V	0.039	0.500
Ti-6Al-4V	0.120	0.520
Ti-13V-11Cr-3Al	0.042	0.465
Ti-13V-11Cr-3Al	0.120	0.520
Ti-6Al-6V-2Sn	0.120	0.520
Ti-2.5Al-11.5Sn 6Zr-1.2Mo-.27Si	0.132	0.475

FIGURE 3 SMOOTH TENSILE SPECIMEN

CYCLIC THERMAL EXPOSURES

For determination of nucleation times under cyclic thermal exposures, the following standard cycle was specified:

1. Heating to test temperature in 10 to 15 minutes.

2. Holding at temperature for three hours.

3. Cooling for 45 to 50 minutes.

Figure 4 shows typical thermal cycles for specimens of sheet and plate tested at 550 and 650F. This cycle was repeated continuously by an automatic programming system. In the case of self-stressed specimens, two of the above cycles were performed each day, and the specimens were stored overnight in a desiccator.

A special cycle (Figure 5) was employed on several specimens of Ti811DA sheet at 550F. This cycle was repeated continuously by an automatic programming system.

X-RAY DIFFRACTION MEASUREMENTS

Hot-stage X-ray diffraction was used on NaCl-coated specimens of titanium-sheet to determine the time required to form $TiCl_2$ at elevated temperatures, and the time for $TiCl_2$ to decompose at room temperature. All measurements were taken using a Norelco diffractometer and copper Kα radiation at 50 Kvp and 20 ma. A sample area of approximately 1/2-inch by 3/4-inch was covered by the X-ray beam.

All specimens were sprayed with a hot NaCl solution to develop a thickness of 0.001 inch of NaCl or 0.002 inch of NaCl which was then microtomed to 0.001 inch. Both techniques produced equivalent test results. The standard 0.002 inch coating could not be utilized because the diffracted X-ray beams were absorbed by the thicker salt layer.

IV RESULTS AND DISCUSSION

MECHANICAL PROPERTIES

Most alloys are more susceptible to stress corrosion in the transverse direction than in the longitudinal direction. Thus, all testing was performed on transverse specimens. Transverse mechanical properties at 450, 550, and 650F are listed in Table IV. The alloys and heat treatments were considered acceptable based on the mechanical properties obtained. Young's modulus data were obtained primarily for calculation of stress levels on self-stressed specimens.

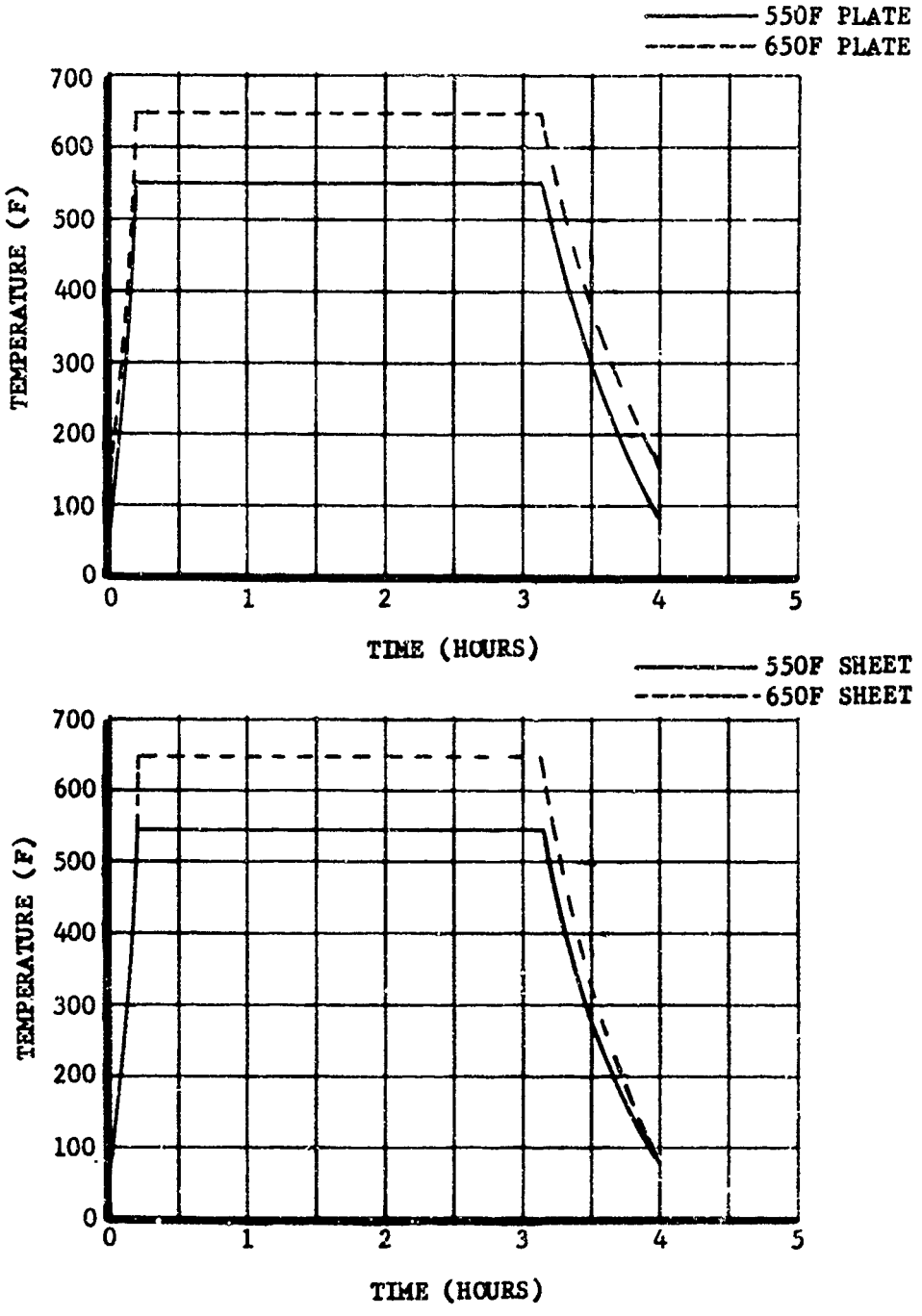

FIGURE 4 TYPICAL STANDARD THERMAL CYCLES FOR SPECIMENS OF SHEET AND PLATE

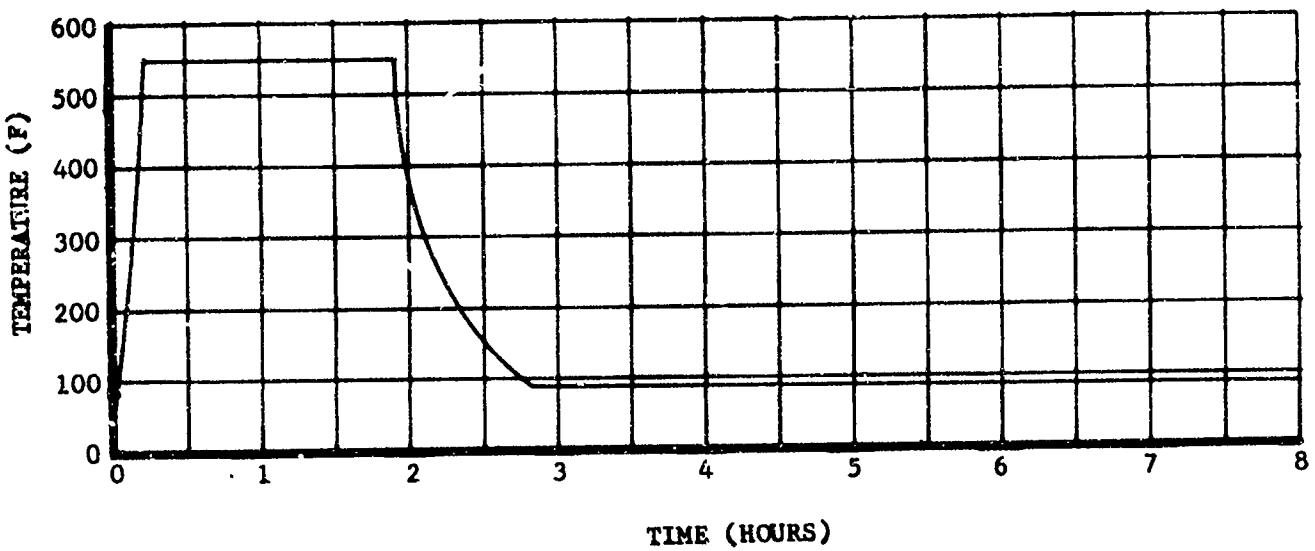

FIGURE 5 SPECIAL THERMAL CYCLE FOR SHEET SPECIMENS OF Ti-8Al-1Mo-1V (DA)

TABLE IV

MECHANICAL PROPERTIES

ALLOY	HEAT TREATMENT	GAGE	YIELD STRENGTH .2% OFFSET (ksi)			ULTIMATE STRENGTH (ksi)			% ELONGATION			YOUNG'S MODULUS X 10^6 (psi)		
			450F	550F	650F	450F	550F	650F	450F	550F	650F	450F	550F	650F
Ti-8Al-1Mo-1V	Mill Annealed	.035	110.6	104.1	101.8	131.6	125.1	124.1	14.0	12.5	11.0	-	-	-
		.125	109.6	103.5	97.9	125.2	121.4	114.3	17.5	17.5	17.0	19.1	17.7	15.6
	Duplex Annealed	.035	107.0	100.0	93.9	126.7	109.2	113.3	11.5	8.0	7.5	17.8	17.9	17.8
		.125	105.7	99.2	94.3	121.4	115.9	111.6	15.5	15.5	15.5	17.1	16.1	13.1
Ti-6Al-4V	Annealed	.040	99.0	90.3	85.0	112.9	105.9	102.2	11.5	10.0	9.0	-	-	-
		.120	115.6	108.5	104.2	126.3	118.5	112.9	12.0	11.0	9.5	19.8	18.8	16.6
	Solution Treated & Aged	.040	120.9	114.8	108.9	-	137.8	132.4	-	7.5	5.0	16.0	15.3	14.5
		.120	130.0	123.3	119.3	150.7	144.7	139	12.5	11.0	8.5	17.4	17.1	16.0
Ti-13V-11Cr-3Al	Annealed	.042	109.2	106.5	106.1	115.0	112.5	113.9	18.5	17.5	20.0	-	-	-
		.121	108.5	107.5	102.0	114.3	113.3	112.5	22.5	18.5	24.0	16.1	16.3	13.4
	Solution Treated & Aged	.042	168.7	165.9	149.7	192.6	190.0	184.8	5.5	5.5	5.0	16.4	16.5	15.6
		.121	157.5	149.4	148.1	179.4	173.9	172.4	6.0	7.0	7.0	16.8	16.0	15.8
Ti-6Al-6V-2Sn	Annealed	.120	131.4	125.3	121.7	149.1	142.7	138.3	14.5	12.5	13.0	17.6	16.5	16.4
	Solution Treated & Aged	.120	143.4	137.0	133.5	158.5	153.2	151.4	12.5	12.5	12.5	16.6	16.1	15.0
Ti-679	Solution Treated & Aged	.133	127.4	119.6	114.7	151.8	144.8	140.4	15.0	15.0	16.0	18.6	16.0	15.4

EDGE-NOTCHED SPECIMENS

The edge-notched and fatigue-cracked specimens tested were of Ti811 alloy primarily, although some testing was performed on the other program alloys. In order to obtain reproducible nucleation times for stress corrosion, it was necessary that the salt be placed at the crack tip. Initially, each specimen was fatigue-cracked, static loaded to open the crack, and saturated salt solution was placed at the notch root. Approximately one hour was required for the salt solution to flow to the tip of the crack by capillary attraction. Surfaces of some specimens were then coated with salt while surfaces of other specimens were left uncoated.

Considerable scatter in stress-corrosion nucleation times was observed for specimens prepared by the above-mentioned method. This was attributed to difficulties in flowing the salt solution to the crack tip in a consistent and reproducible manner. Therefore, a new procedure was adopted. A drop of NaCl solution was placed at the notch and pumped into the existing fatigue crack by cycling between a 1 and 5 ksi net-section stress. Salt solution was placed at the crack tip very effectively using this procedure, which was employed for all subsequent tests.

Typical results of visual and fractographic analyses are shown in Figures 6 and 7 for Ti811DA sheet and plate specimens tested at 800F. In all cases, the fatigue cracks were typified by regularly-spaced fatigue striations. Salt at the crack tip produced a stress-corrosion crack-extension easily identified by the presence of a dark band just beyond the fatigue-crack front. Formation of this band was characterized by an initial crack extension of approximately 0.004 to 0.01 inch which was defined as stress-corrosion nucleation. However, after the initial crack extension, further growth of the crack became very slow. Presumably, this occurred because solid salt was not effectively transported to the tip of the crack. This type of behavior was observed in specimens containing salt in the cracks as well as specimens which contained salt on the surfaces and in the cracks. Stress corrosion tests at 550F and 650F produced similar results.

Fractographs of the dark bands just beyond the fatigue cracks show transgranular cleavage-type fracture typified by planar cleavage facets. This fracture topology apparently characterizes hot-salt stress corrosion of Ti811DA. This fracture topology is also shown (Figure 6) in the area where surface salt had produced severe inward stress corrosion. These fractographs show no evidence of corrosion-product formation in the dark bands just beyond the fatigue cracks. It is believed that the low quantity of salt at the crack tip could not produce corrosion products visible at this magnification, since a heavy formation of corrosion products was observed in the stress-corrosion regions initiating from the salt-coated surfaces (Figure 6).

The stress-corrosion fracture topology was not comparable to notch-initiated fractures which normally show a transgranular, dimpled structure for this alloy[4]. In addition, this topology was not caused by oxidation alone since one fatigue-cracked plate sample with no salt was exposed for 30 hours at 800F at a net-section stress of 15 ksi. No evidence of crack

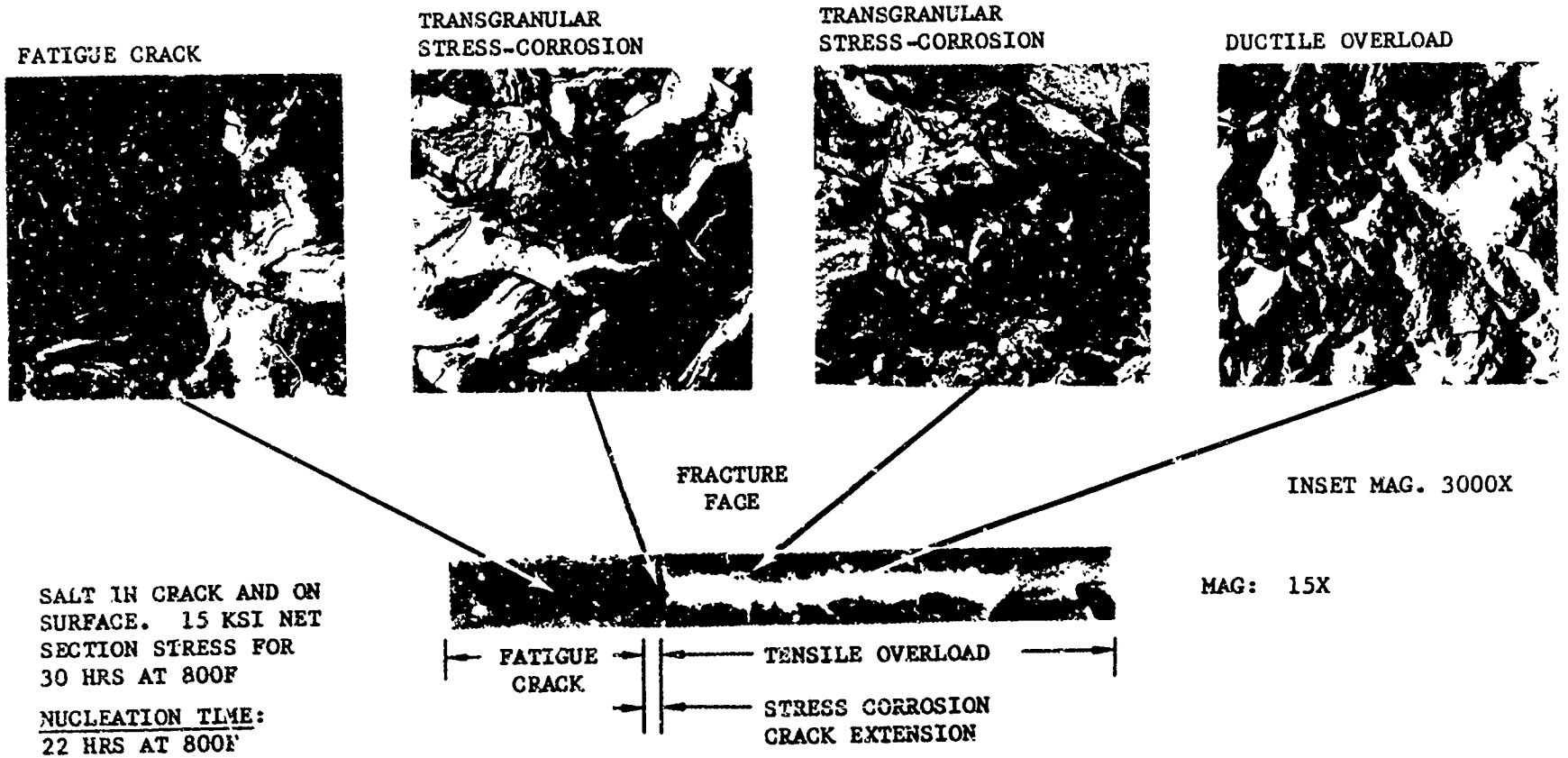

FIGURE 6 FRACTOGRAPHIC ANALYSIS OF HOT-SALT STRESS-CORROSION CRACKING OF Ti-8Al-1Mo-1V DUPLEX-ANNEALED SHEET

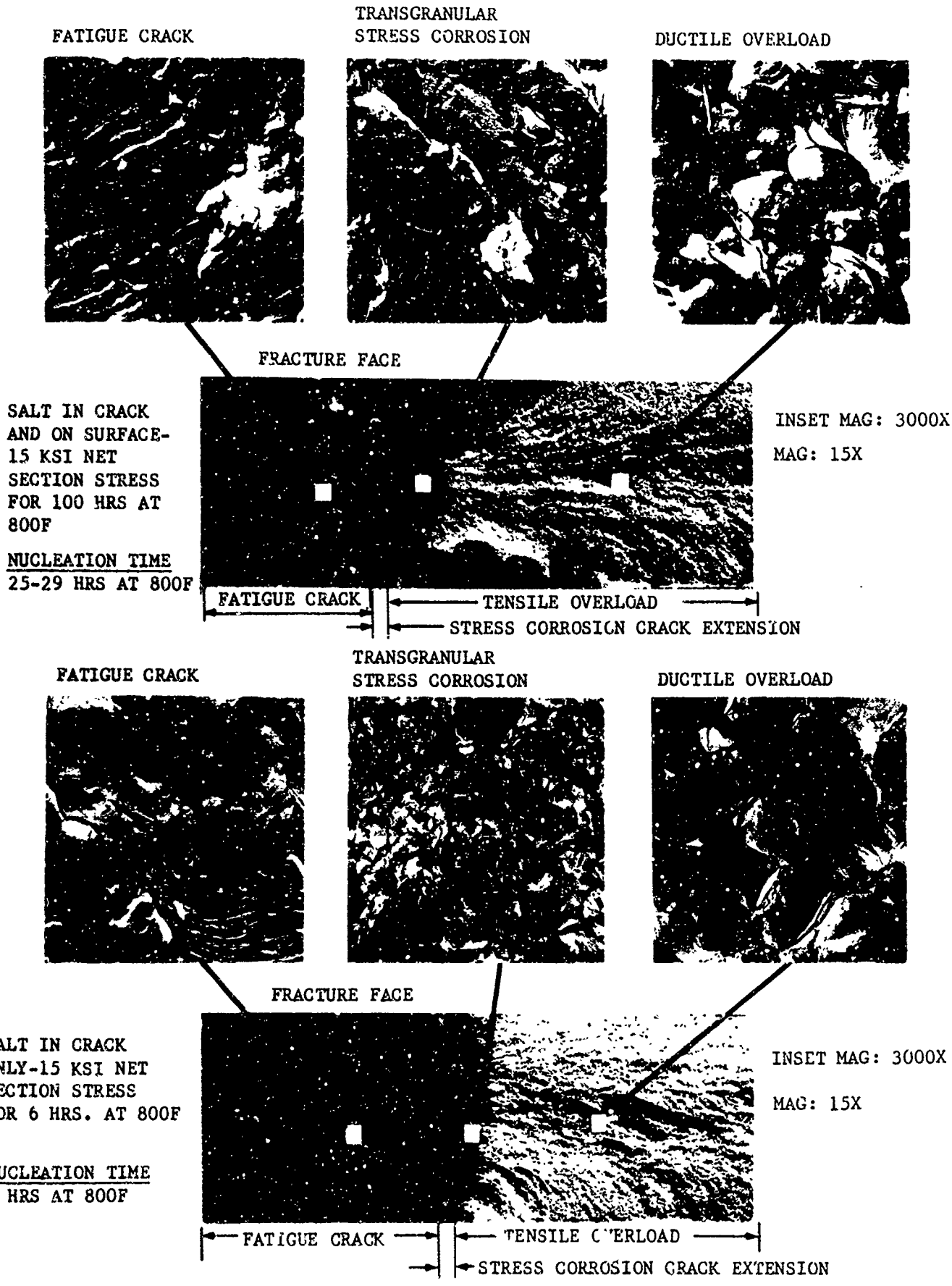

FIGURE 7 FRACTOGRAPHIC ANALYSIS OF HOT-SALT STRESS-CORROSION CRACKING OF Ti-8Al-1Mo-1V DUPLEX-ANNEALED PLATE

extension or of the dark stress-corrosion band was observed.

Additional specimens with and without salt at the crack tip were coated with 0.002 inch of NaCl and exposed in the 550F to 800F range. Results of these tests led to several conclusions concerning the use of fatigue-cracked specimens to determine stress-corrosion nucleation times. These conclusions are as follows:

1. Salt on the surface alone produced no growth of the existing fatigue crack, but did produce nucleation and growth of surface stress corrosion cracks in the high stress region near the crack tip. Since the stress field varied in this region, it was difficult to correlate crack-nucleation time with stress level.

2. Salt on the surface and at the crack tip produced growth of the existing fatigue crack by stress corrosion and the formation of new surface cracks as discussed above. The nucleation and growth of new surface cracks produced a greater loss in net-section area than growth of the existing fatigue crack.

3. Salt at the crack tip alone produced an initial growth of the fatigue crack by stress corrosion. However, times required to produce this growth were not reproducible. After 0.004 - 0.010 inch of crack growth, the growth rate decreased very substantially because the salt was not transported to the crack tip. Thus, the corrosive environment at the crack tip was not constant.

The approaches employing salt on the surface are not controlled by fracture mechanics, i.e., only growth of the existing fatigue crack, because additional surface cracks nucleate and grow independent of the existing crack. The approach with salt at the crack tip alone follows fracture mechanics, but experimental problems produced a high degree of scatter in nucleation times. A real structure in service would undoubtedly have salt on the surface and in existing cracks. Thus, loss of load carrying ability would be dependent primarily upon loss of net-section area caused by nucleation and growth of new surface cracks and not growth of an existing crack by stress-corrosion.

Since the above observations show that hot-salt stress corrosion of titanium alloys is not controlled by fracture mechanics, use of fatigue-cracked specimens is not necessary and, indeed, is inadvisable because of poor test reproducibility. Therefore, smooth tensile specimens were employed for the remainder of this program.

SELF-STRESSED SHEET SPECIMENS

Stress-corrosion nucleation times obtained under continuous thermal exposure at 450F are summarized in Table V. The Ti811MA sheet stressed at 95 ksi exhibited a stress-corrosion nucleation time of 1000-1500 hours. The remaining alloys showed no stress corrosion after 2550 hours of exposure at stresses of approximately 60%-90% of their yield strengths at 450F. Since these data indicated that hot-salt stress-corrosion cracking was not a significant problem at 450F, further testing was concentrated at 550F and 650F where the problem was potentially more severe.

TABLE V

CONTINUOUS STRESS-CORROSION NUCLEATION TIMES
AT 450F ON SELF-STRESSED SHEET

ALLOY (1)	TEST STRESS (ksi)	APPROXIMATE PERCENTAGE OF 450F YIELD STRENGTH	NUCLEATION TIME (hours)
Ti64STA	80	65	>2550
	95	80	>2550
Ti64A	80	80	>2550
Ti811DA	80	75	>2550
	95	90	>2550
Ti811MA	80	70	>2550
	95	85	1000-1500
B120STA	120	70	>2550
	140	85	>2550
B120A	80	75	>2550
	95	90	>2550

NOTE: (1) STA - Solution Treated and Aged
A - Annealed
DA - Duplex Annealed
MA - Mill Annealed

Table VI shows the stress-corrosion nucleation times obtained under continuous thermal exposures and the specified, standard, cyclic thermal exposures at 650F. In general, continuous nucleation times were longer than a single Mach 3 mission, but several orders of magnitude shorter than the overall design life of a Mach 3 aircraft. With the exception of B120 in both heat-treat conditions, the cyclic nucleation times were essentially equivalent to the continuous nucleation times. The cyclic nucleation times for B120STA and B120A at 40 ksi are highly stress dependent and this suggested that a decrease in test-stress levels for all program alloys would show larger differences between cyclic and continuous nucleation times.

SMOOTH TENSILE SPECIMENS

Smooth tensile specimens of sheet and plate were employed for the majority of tests on this program rather than self-stressed specimens. Dead-weight-loaded tensile specimens offered the advantages of more accurately defined stresses, elimination of stress changes caused by relaxation, and a cross-section at a constant stress rather than a varying stress.

Several tests were conducted under continuous thermal exposure at 650F to determine stress-corrosion nucleation times as a function of rolling direction. Plate specimens of Ti811DA exposed at 70 ksi exhibited stress-corrosion nucleation times of 28 hours and less than 6 hours in the longitudinal and transverse directions, respectively. Plate specimens of Ti64STA exposed at 60 ksi exhibited nucleation times of 11 hours and less than 6 hours in the longitudinal and transverse directions, respectively. These limited data showed that hot-salt stress corrosion occurred more rapidly in the transverse direction than the longitudinal direction, which is typical of a large number of stress corrosion processes. Therefore, all further tests on smooth specimens were conducted on transverse specimens to represent the worst conditions.

Stress-corrosion nucleation times are shown in Figures 8 through 15 for continuous thermal exposure and the specified, cyclic, thermal exposure. Nucleation times are plotted as a function of the ratio of test stress (σ_{sc}) to yield strength (σ_{ys}) at 550F and 650F in order to normalize differences in strength levels of various alloys. On these curves, points with arrows pointing to the left indicate specimens which exhibited relatively large cracks and were therefore exposed beyond the nucleation time. An arrow to the right indicates that no cracking had occurred at the time indicated. Many data points from early tests which did not contribute to a close definition of nucleation times were omitted to make these figures clearer.

In general, the data in these figures were only in fair agreement with comparable results obtained on self-stressed specimens. However, the data for self-stressed specimens were considered less accurate because loading conditions were not as well defined as they were for the smooth-tensile specimens. In addition, the thermal cycles for self-stressed and smooth specimens were somewhat different. Self-stressed specimens were held overnight at room temperature whereas smooth specimens were cycled continuously.

Figures 9, 11, 13, 14, and 15 show that most of the alloys tested at 650F exhibited continuous nucleation times of 10 hours or less at σ_{sc}/σ_{ys} ratios as low as 0.5. Thus, nucleation of stress corrosion cracks at 650F was very rapid and, in many cases, well within the time-at-temperature of a single Mach 3 mission. At 550F (Figures 8, 10, 12, 14, and 15) and σ_{sc}/σ_{ys} ratios of 0.5 or less, continuous nucleation times were generally greater than

TABLE VI

CONTINUOUS AND CYCLIC STRESS-CORROSION NUCLEATION TIMES AT 650F ON SELF-STRESSED SHEET

ALLOY(1)	TEST STRESS (ksi)	APPROXIMATE PERCENTAGE OF 650F YIELD STRENGTH	CONTINUOUS NUCLEATION TIME (hours)	CYCLIC(2) NUCLEATION TIME (TIME AT TEMP.)(hours)
Ti64STA	60	55	52.5 ± 2.5	51
	80	70	23 ± 2	Between 21-111
Ti64A	60	70	70 ± 2	72
	75	90	9 ± 1	Between 9-45
Ti811DA	60	65	52.5 ± 2.5	51
	80	85	23 ± 2	21
Ti811MA	60	60	7 ± 1	6
	80	75	7 ± 1	6
B120STA	40	25	22.5 ± 2.5	>210
	80	50	Less than 1	
	120	75	Less than 1	
B120A	40	40	96	>210
	60	60	Less than 1	
	80	80	Less than 1	

NOTES: (1) STA - Solution Treated and Aged
A - Annealed
DA - Duplex Annealed
MA - Mill Annealed

(2) Thermal Cycle:
a. Heating to 650F in 10-15 minutes
b. Holding at 650F for three hours
c. Cooling for 45-50 minutes

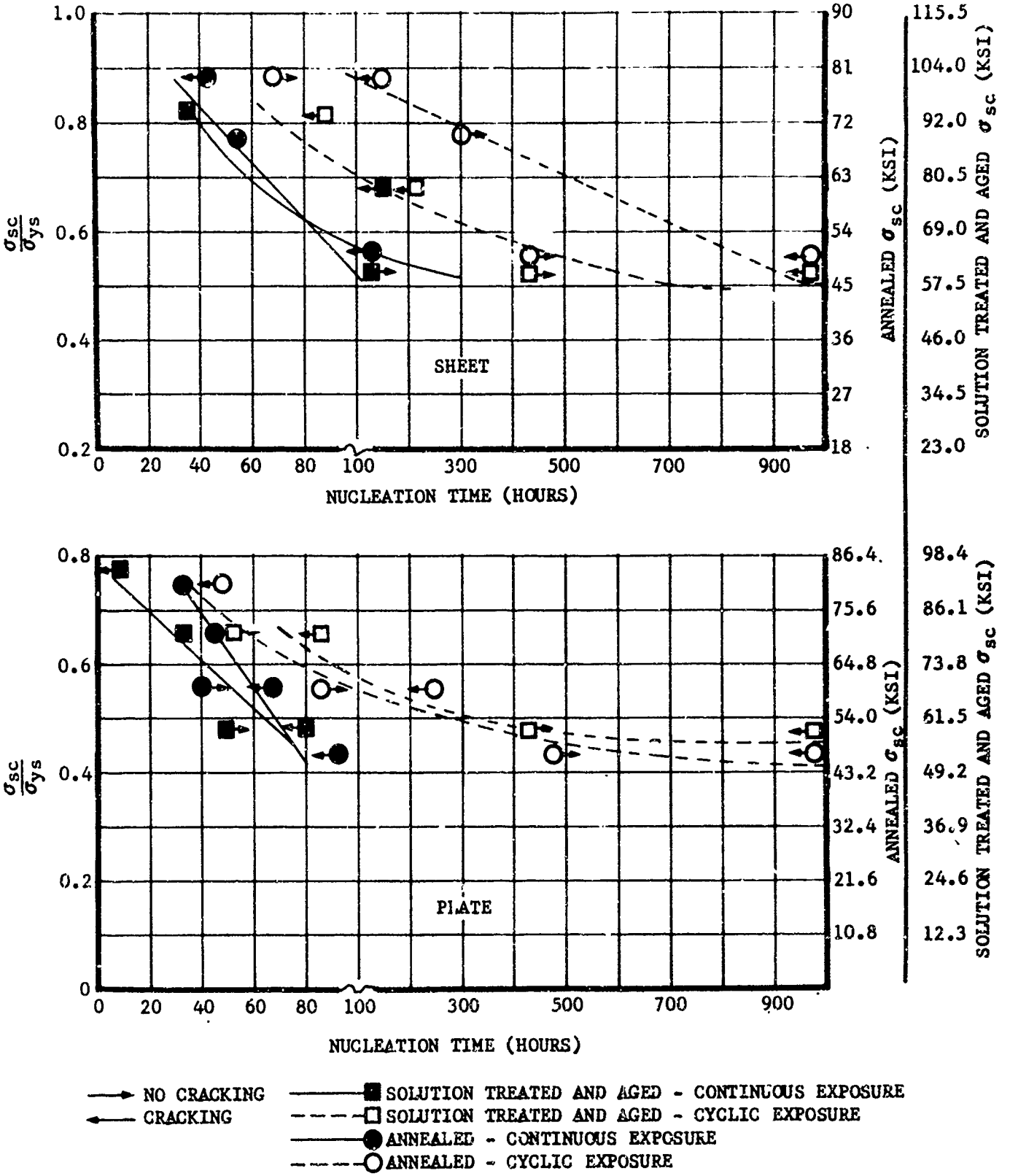

FIGURE 8 CONTINUOUS AND CYCLIC NUCLEATION TIMES FOR HOT-SALT STRESS-CORROSION CRACKING OF Ti-6Al-4V AT 550F

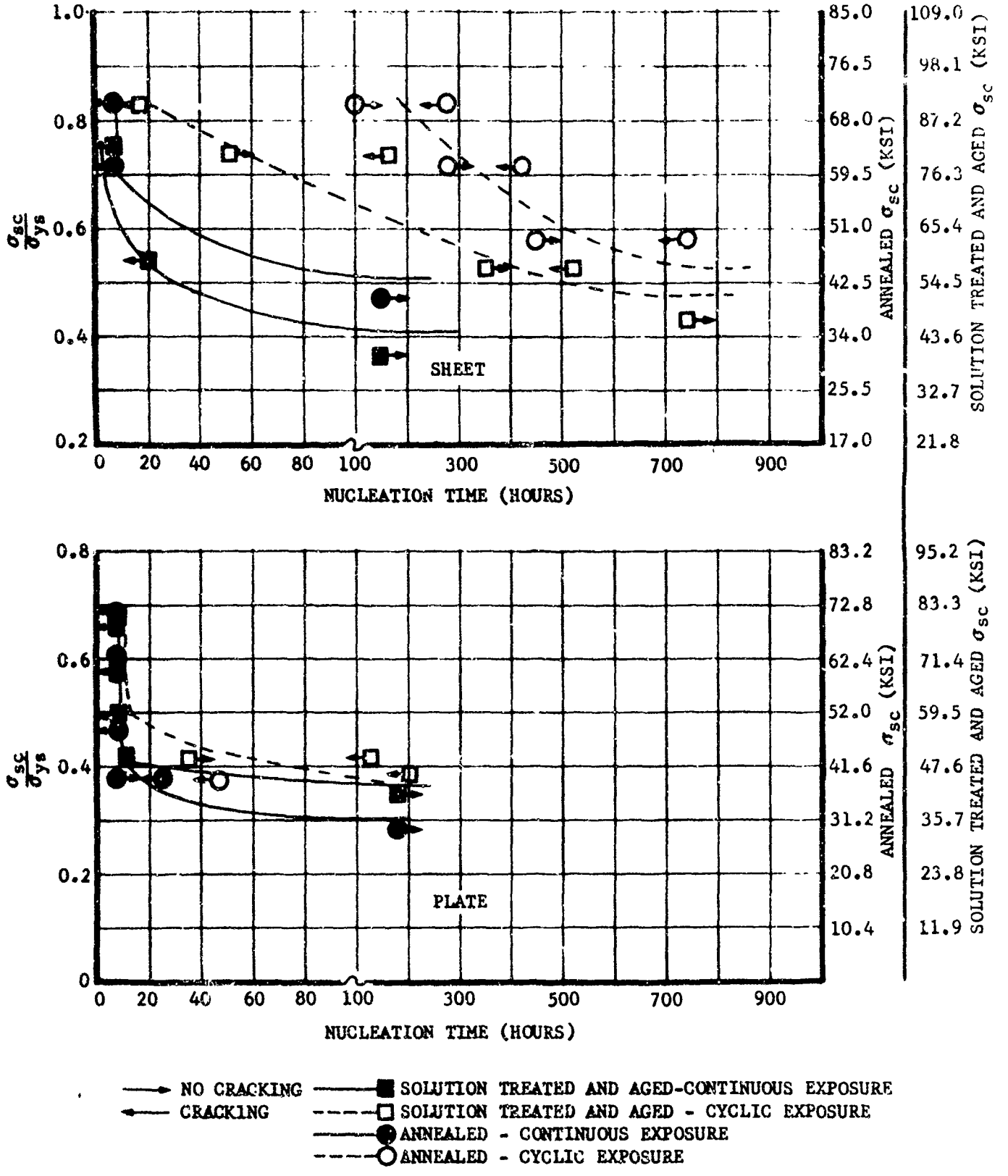

FIGURE 9 CONTINUOUS AND CYCLIC NUCLEATION TIMES FOR HOT-SALT STRESS-CORROSION CRACKING OF Ti-6Al-4V AT 650F

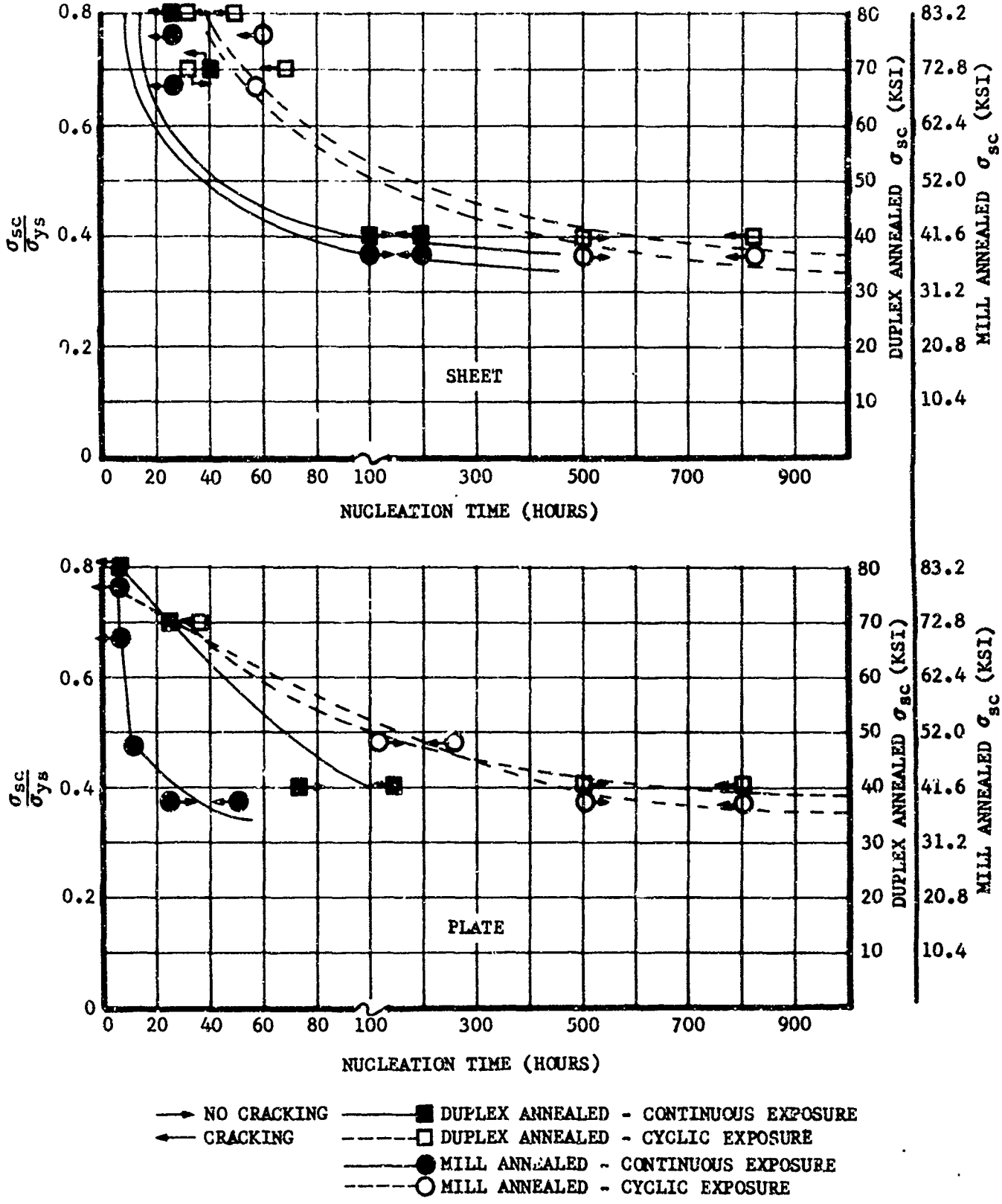

FIGURE 10 CONTINUOUS AND CYCLIC NUCLEATION TIMES FOR HOT-SALT STRESS-CORROSION CRACKING OF Ti-8Al-1Mo-1V AT 550F

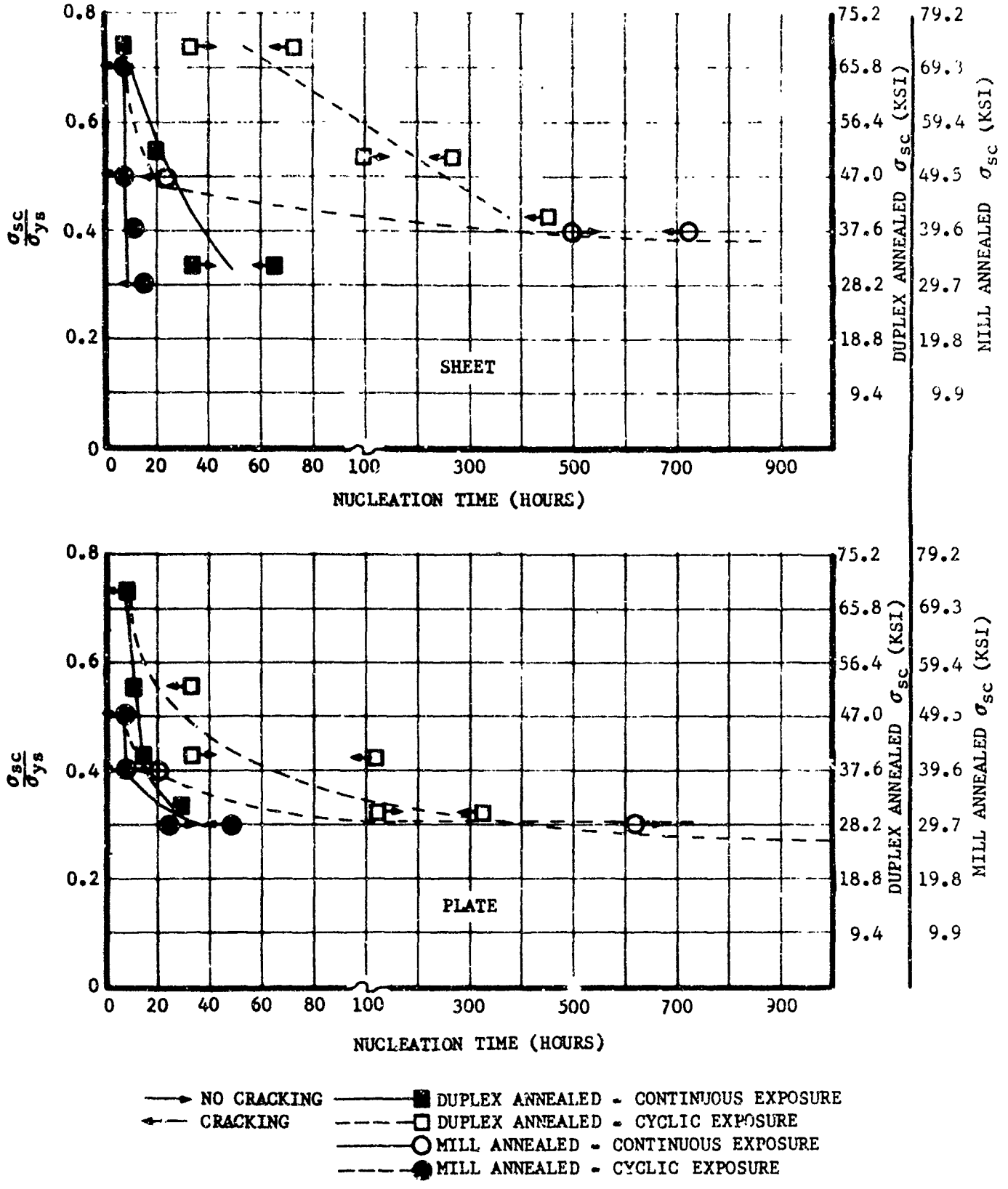

FIGURE 11 CONTINUOUS AND CYCLIC NUCLEATION TIMES FOR HOT-SALT STRESS-CORROSION CRACKING OF Ti-8Al-1Mo-1V AT 650F

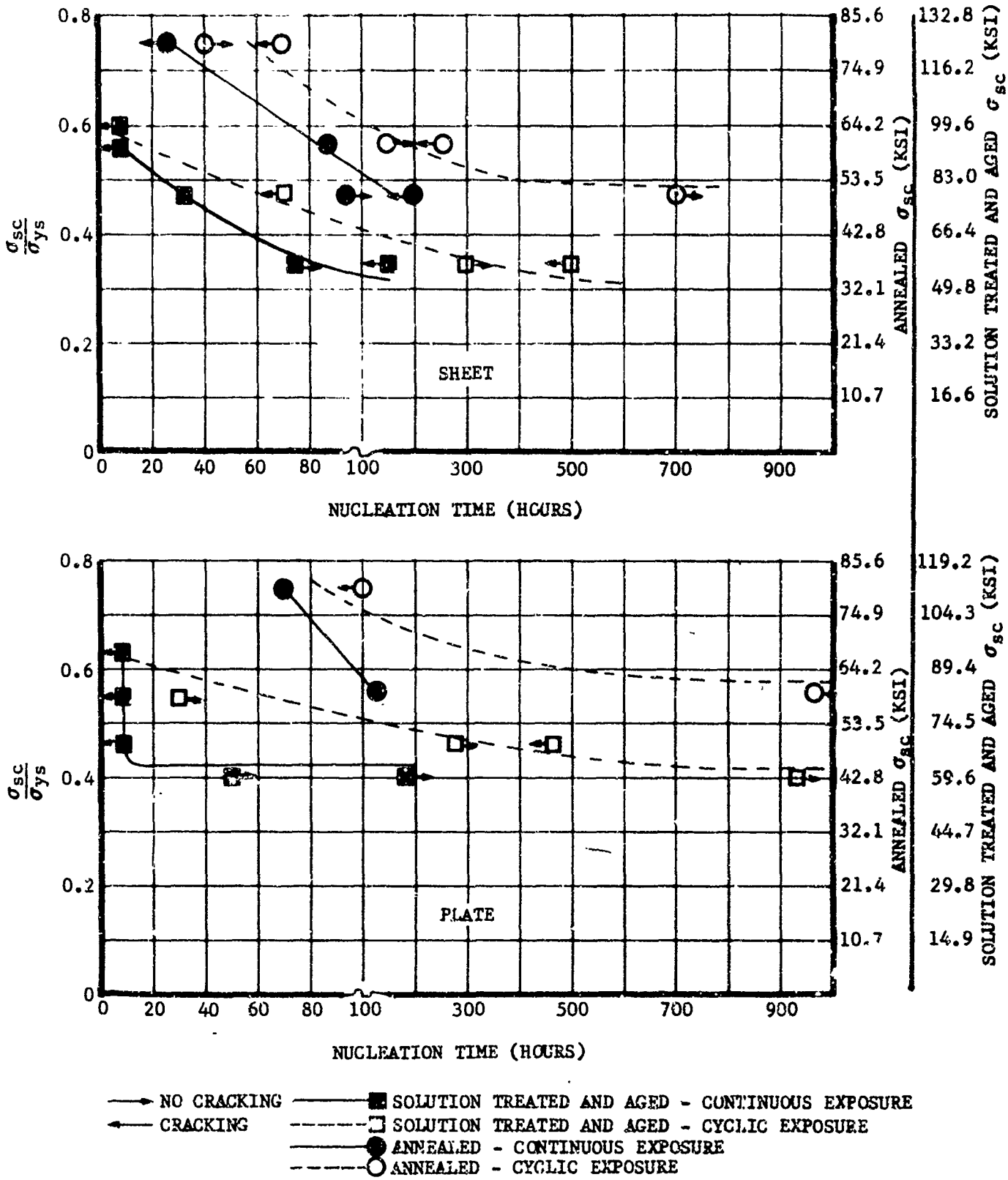

FIGURE 12 CONTINUOUS AND CYCLIC NUCLEATION TIMES FOR HOT-SALT STRESS-CORROSION CRACKING OF Ti-13V-11Cr-3Al (B120) AT 550F

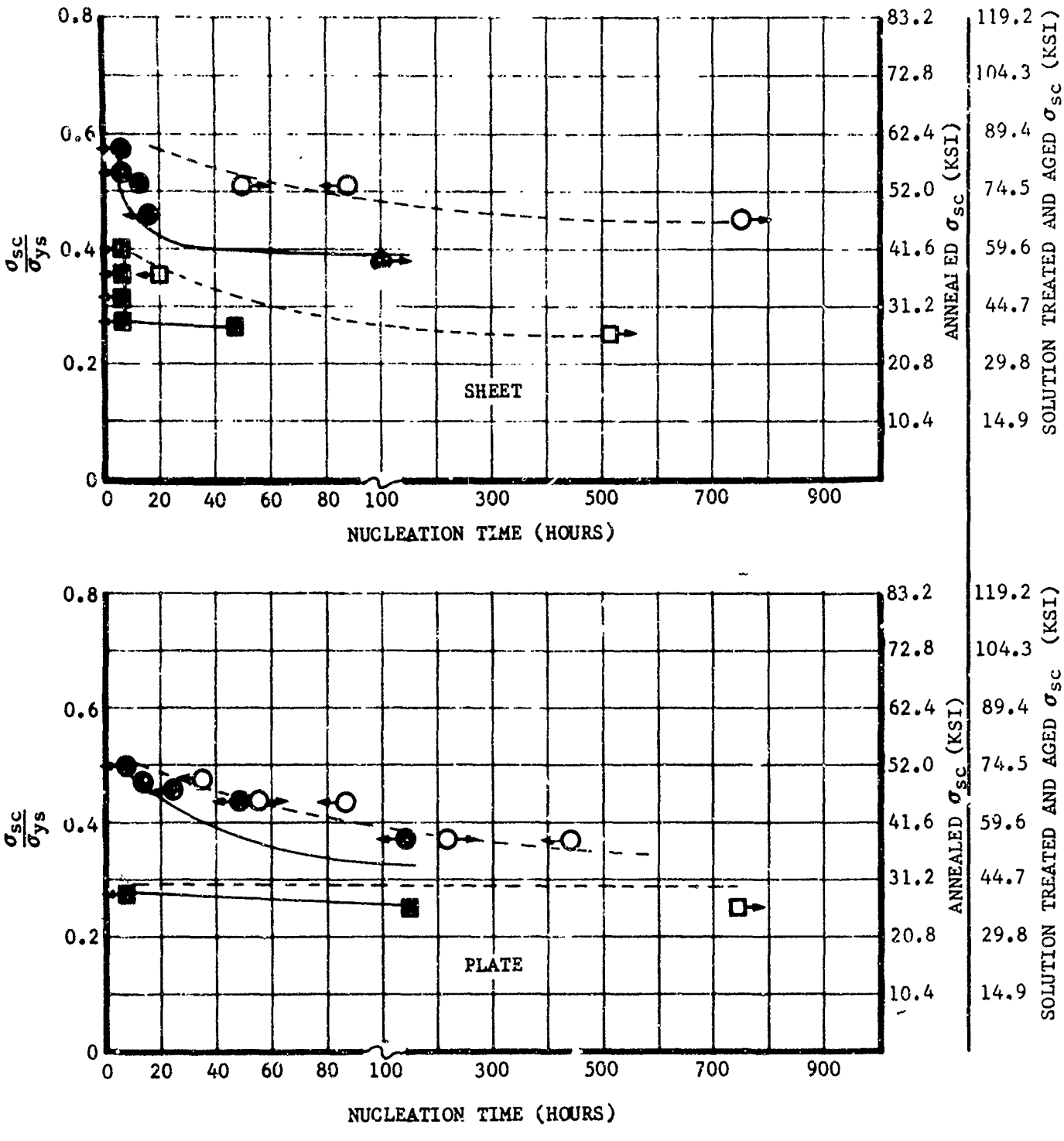

FIGURE 13 CONTINUOUS AND CYCLIC NUCLEATION TIMES FOR HOT-SALT STRESS-CORROSION CRACKING OF Ti-13V-11Cr-3Al (B120) AT 650F

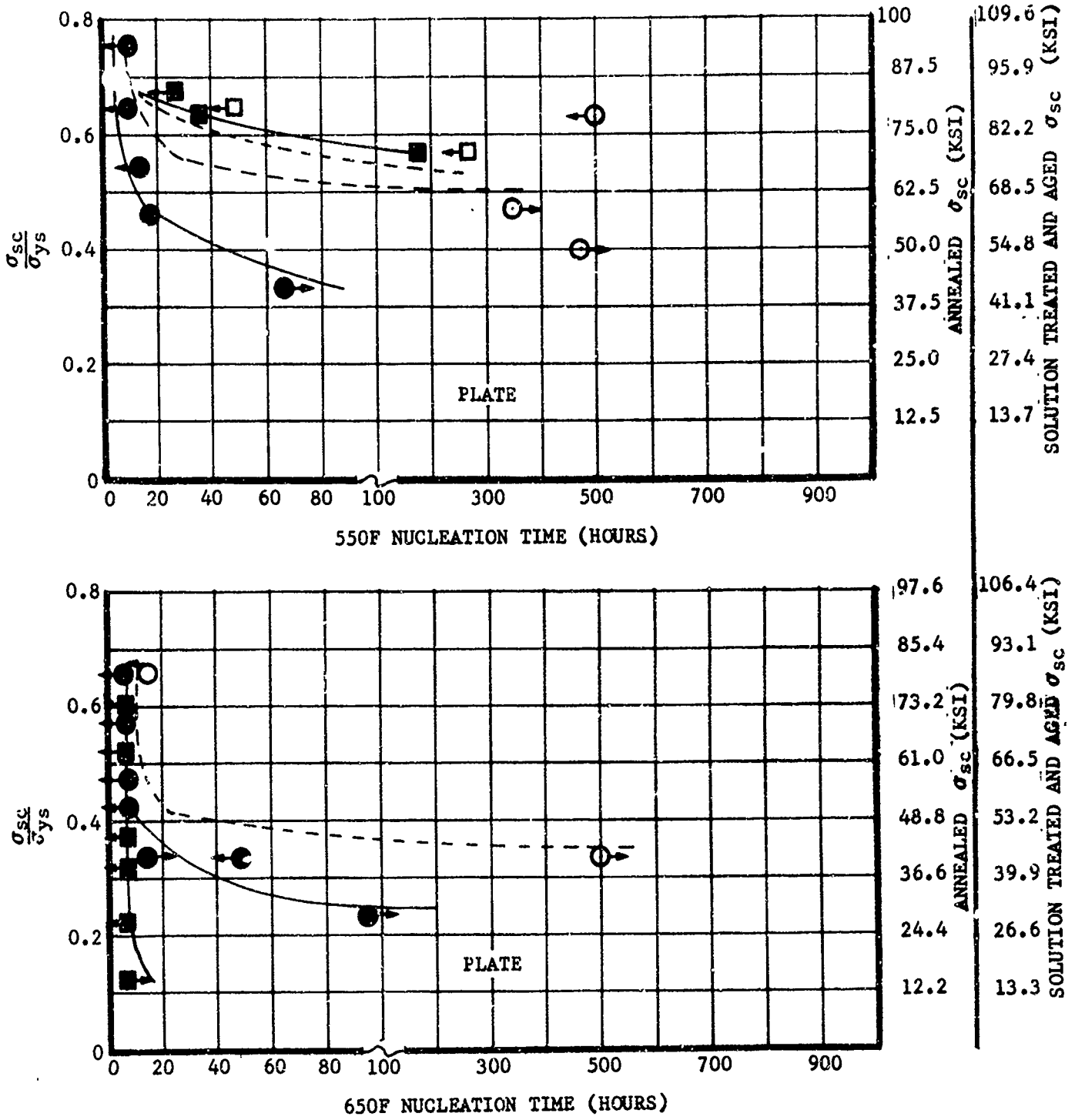

FIGURE 14 CONTINUOUS AND CYCLIC NUCLEATION TIMES FOR HOT-SALT STRESS-CORROSION CRACKING OF Ti-6Al-4V-2Sn

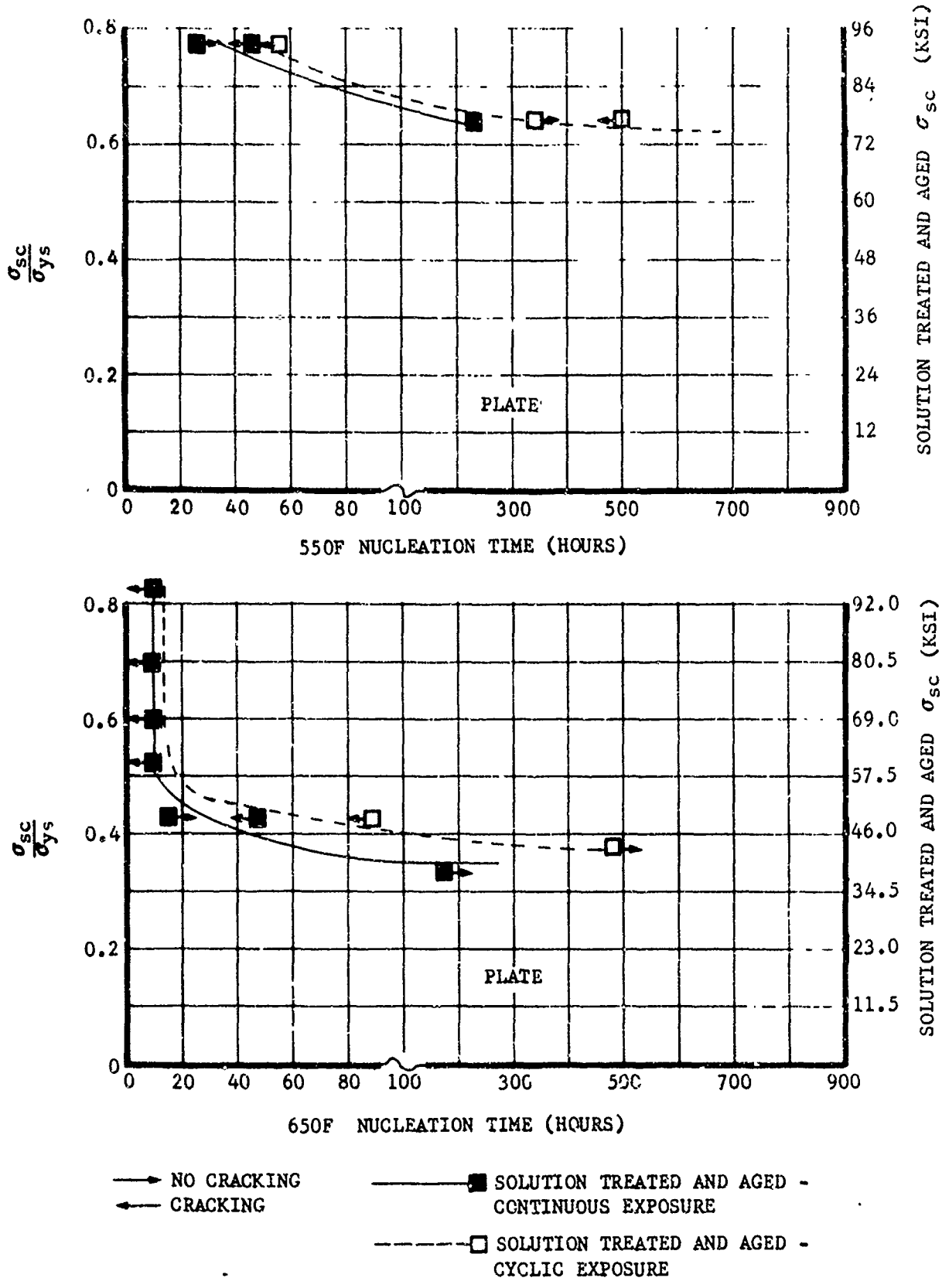

FIGURE 15 CONTINUOUS AND CYCLIC NUCLEATION TIMES FOR HOT-SALT STRESS-CORROSION CRACKING OF Ti-679

a single Mach 3 mission, but several orders of magnitude less than the design life of a Mach 3 aircraft. At higher σ_{sc}/σ_{ys} ratios, continuous nucleation times varied greatly depending upon the specific alloy, its heat treatment, and its gage; nucleation times for some alloys were less than a single Mach 3 mission; whereas, other alloys exhibited longer nucleation times.

No general trends were observed in continuous nucleation times as a function of material thickness in the Ti811 and B120 alloys. At 550F and 650F, the Ti64 alloy in plate form exhibited shorter continuous nucleation times than sheet in both heat treat conditions. However, the differences between nucleation times for sheet and plate specimens of a specific alloy were relatively small.

Heat treatment produced significant effects on continuous nucleation times at 550F and 650F. Figures 8 and 9 show that stress-corrosion cracks generally nucleated more rapidly in Ti64STA than in Ti64A. Similarly, Ti811MA exhibited shorter nucleation times than Ti811DA (Figures 10 and 11). Figures 12 and 13 show that nucleation times for B120STA were considerably shorter than for B120A. At 550F, Ti662A exhibited much shorter nucleation times than Ti662STA, but this trend was reversed at 650F (Figure 14).

Differences between continuous and cyclic nucleation times depended upon the specific alloy and its condition. Cyclic nucleation times were substantially longer than continuous nucleation times at σ_{sc}/σ_{ys} ratios in the range of 0.3 to 0.6. At ratios above approximately 0.6, cyclic and continuous nucleation times were essentially equivalent. Several exceptions which still showed significantly longer cyclic nucleation times well above a ratio of 0.6 were the following:

Ti64STA Sheet	550 and 650F	(Figures 8 and 9)
Ti64A Sheet	550 and 650F	(Figures 8 and 9)
Ti811DA Sheet	550F	(Figure 10)
Ti811MA Sheet	550F	(Figure 10)
Ti811DA Sheet	650F	(Figure 11)

Figures 8 through 15 showed a strong trend toward the development of threshold σ_{sc}/σ_{ys} ratios below which stress corrosion would not occur under continuous or cyclic thermal exposures. Approximate threshold ratios for stress corrosion are summarized in Table VII. In most cases, there was no significant difference between the threshold σ_{sc}/σ_{ys} ratios for continuous and cyclic exposures. Only Ti662A plate tested at 550F and 650F (Figure 14) and Ti811MA sheet tested at 650F (Figure 11) had cyclic threshold-ratios that were somewhat higher than continuous threshold-ratios. For most of the alloys, threshold ratios under cyclic and continuous exposures fell within the bands of 0.35 to 0.50 at 550F and 0.25 to 0.45 at 650F. Thus, as the test temperature was increased from 550F to 650F, the threshold ratios decreased only moderately.

TABLE VII

APPROXIMATE THRESHOLD STRESS RATIOS (σ_{sc}/σ_{ys}) FOR STRESS-CORROSION CRACKING

ALLOY AND FORM	550F		650F	
	CONTINUOUS EXPOSURE	CYCLIC EXPOSURE	CONTINUOUS EXPOSURE	CYCLIC EXPOSURE
T164STA Sheet	~ .52	.50	.42	.49
T164A Sheet	< .52	.50	.51	.54
T164STA Plate	< .46	.46	.37	.37
T164A Plate	< .44	.43	.31	~ .31
T1811DA Sheet	~ .37	.38	< .32	< .42
T1811MA Sheet	.34	.36	< .30	.39
T1811DA Plate	< .40	.38	< .33	.29
T1811MA Plate	< .35	.36	< .30	.30
B120STA Sheet	< .31	~ .30	.26	.26
B120A Sheet	< .45	.49	.39	.45
B120STA Plate	.42	.42	.26	.28
B120A Plate	< .55	.57	~ .33	.36
T1662STA Plate	< .58	< .58	< .12	< .20
T1662A Plate	~ .30	.50	.24	.35
T1679STA Plate	~ .62	~ .62	.36	.38

Stress-corrosion susceptibility ratings for the program materials were determined based upon threshold loading conditions for stress corrosion under cyclic thermal exposures at 550F and 650F. Since threshold levels were almost identical under continuous and cyclic exposures, the ratings were essentially the same for either case. Ratings based upon threshold σ_{sc}/σ_{ys} ratios are shown in Table VIII. At 550F, Ti679STA plate and B120A plate were least susceptible to stress corrosion; B120STA sheet and Ti811 sheet and plate in both heat-treat conditions were most susceptible. At 650F, the susceptibility ratings changed significantly; Ti64A sheet was least susceptible to stress corrosion and Ti622STA plate was most susceptible.

Stress-corrosion susceptibility ratings were also determined based upon threshold stress levels (σ_{sc}), as shown in Table IX. This rating system did not change relative positions of alloys substantially, except for B120STA sheet and plate. The high strength of this alloy resulted in low stress-corrosion susceptibility based upon a threshold σ_{sc} rating, but a high susceptibility based upon a threshold σ_{sc}/σ_{ys} rating.

The above rating methods, based upon threshold loading conditions, show no beneficial effects from the thermal cycle used in this program. At loading conditions below threshold levels, stress corrosion cracking did not occur under continuous or cyclic exposures. However, at loading conditions just above the threshold levels, cyclic exposures produced a substantial increase in stress-corrosion nucleation times in most cases. At higher loading conditions, there was no benefit from cyclic exposures because continuous and cyclic nucleation times were essentially equivalent. Therefore, the thermal cycle used in this program reduced stress corrosion cracking only within a region of moderate stresses. If higher sustained stresses are encountered in a typical Mach 3 titanium aircraft structure operating at 550F to 650F, the thermal cycle of this program would produce no major reduction in hot-salt stress-corrosion cracking.

WELDED SPECIMENS

The continuous and cyclic nucleation times obtained for welded specimens of Ti811DA and Ti64STA are compared with those for parent materials tested at the same stresses and temperatures (Table X). Welding produced no detrimental effects on the stress corrosion behavior of the Ti811DA and Ti64STA. At 550F, the weldments exhibited longer continuous nucleation time than parent materials. At 650F, continuous nucleation times for welds were equal to or slightly

longer than nucleation times for parent materials, with one exception. The Ti64STA welded with Ti64 filler exhibited substantially longer continuous nucleation times than parent material. Comparison of cyclic nucleation for weldments and parent materials showed the welds to exhibit substantially longer cyclic nucleation times than parent materials, particularly at 650F. These results indicated that, based upon nucleation behavior, the most stress-corrosion-sensitive region of weldments on these alloys was the parent material.

In contrast, Turley and Avery[5] and Newcomer, Tourkakis, and Turner[6] conducted very limited hot-salt (ASTM synthetic sea salt) stress corrosion tests at 600, 700, and 800F on welded and stress-relieved specimens of Ti64A and Ti811 (triplex annealed). Both investigations showed that welded and stress-relieved specimens exhibited lower stress-corrosion threshold stresses than parent material specimens. Turley and Avery[5] said that, "Since the weld zone or heat-affected zone was not always the initiation point of stress-corrosion fracture and yet welded specimen threshold stresses were lower than those for the basic material, we consider it likely that the stress relief treatment was the major factor in lowering threshold stresses of the welded specimens." The results of Newcomer, Tourkakis, and Turner[6] showed the same type of behavior.

Results of this investigation were considerably different than the results of the studies mentioned above. These latter results were obtained from specimens which were stress relieved after welding with no machining of the weld bead. In this investigation, no post-weld stress relief was employed, and the weld bead was milled flush with the base alloy. Approximately 0.002 inch was also removed simultaneously from the heat-affected zone and adjacent base alloy during the milling operation.

It would not be expected that all of the microstructures represented by the fusion and heat-affected zones would be less susceptible to stress corrosion than parent material. However, the welded specimens did in fact exhibit lower stress corrosion susceptibility than parent material. It is possible that machining produced residual surface compressive stresses which decreased stress corrosion susceptibility. Additional tests are required to verify this hypothesis.

TABLE VIII

STRESS-CORROSION SUSCEPTIBILITY OF TITANIUM ALLOYS

BASED UPON CYCLIC THRESHOLD-STRESS RATIOS

550F			650F		
ALLOY		CYCLIC THRESHOLD $\frac{\sigma_{sc}}{\sigma_{ys}}$	ALLOY		CYCLIC THRESHOLD $\frac{\sigma_{sc}}{\sigma_{ys}}$
Ti679STA	Plate	~ .62	Ti164A	Sheet	.54
B120A	Plate	.57	Ti164STA	Sheet	.49
Ti164STA	Sheet	.50	B120A	Sheet	.45
Ti164A	Sheet	.50	Ti811MA	Sheet	.39
Ti662A	Plate	.50	Ti679STA	Plate	.38
Ti662STA	Plate	< .58	Ti164STA	Plate	.37
B120A	Sheet	.49	B120A	Plate	.36
Ti164STA	Plate	.46	Ti662A	Plate	.35
Ti164A	Plate	.43	Ti164A	Plate	~ .31
B120STA	Plate	.42	Ti811MA	Plate	.30
Ti811DA	Sheet	.38	Ti811DA	Plate	.29
Ti811DA	Plate	.38	Ti811DA	Sheet	< .42
Ti811MA	Sheet	.36	B120STA	Plate	.28
Ti811MA	Plate	.36	B120STA	Sheet	.26
B120STA	Sheet	~ .30	Ti662STA	Plate	< .20

Increasing Susceptibility to Stress Corrosion

TABLE IX

STRESS-CORROSION SUSCEPTIBILITY OF TITANIUM ALLOYS
BASED UPON CYCLIC THRESHOLD STRESSES

550F		650F	
ALLOY	CYCLIC THRESHOLD STRESS (ksi)	ALLOY	CYCLIC THRESHOLD STRESS (ksi)
Ti679STA Plate	74	Ti164STA Sheet	53
Ti662STA Plate	< 79.5	Ti164A Sheet	47
B120STA Plate	62.5	B120A Sheet	47
Ti662A Plate	62.5	Ti164STA Plate	44
B120A Plate	61	Ti679STA Plate	43.5
Ti164STA Sheet	57.5	Ti662A Plate	42.5
Ti164STA Plate	56.5	B120STA Plate	42
B120A Sheet	52	Ti811MA Sheet	39
B120STA Sheet	~ 50	B120STA Sheet	39
Ti164A Plate	46.5	B120A Plate	37
Ti164A Sheet	45	Ti164A Plate	~ 32
Ti811DA Sheet	38	Ti811MA Plate	30
Ti811DA Plate	38	Ti811DA Plate	27
Ti811MA Sheet	37	Ti811DA Sheet	< 39
Ti811MA Plate	37	Ti662STA Plate	< 26.5

Increasing Susceptibility
To Stress Corrosion

TABLE X

STRESS-CORROSION NUCLEATION TIMES AT
550F AND 650F ON WELDED PLATE SPECIMENS

ALLOY	FILLER WIRE	TEST STRESS (ksi)	σ_{sc}/σ_{ys} (1)	CONTINUOUS NUCLEATION TIME (hours)	CYCLIC NUCLEATION TIME (hours)	CONTINUOUS NUCLEATION TIME (hours)	CYCLIC NUCLEATION TIME (hours)
		550F		Welded Plate Specimens		Parent Material Plate Specimens	
T1811DA	T175A	70	.7	> 400	-	24	< 36
		80	.8	> 100	-	< 6	< 6(5)
T1811DA	T1811	70	.7	Between 200 & 400 (FZ)(2)	> 700	24	< 36
		80	.8	15 ± 9 (FZ)(2)	> 200	< 6	< 6(5)
T164STA	T175A	80	.65	> 400	-	32	70
T164STA	T164	80	.65	> 400	-	32	70
		95	.78	> 100	-	< 6	< 6(5)
		650F					
T1811DA	T175A	50	.53	15 ± 9 (HAZ)(3)	> 400	10	< 32
		70	.75	15 ± 9 (FZ)(3)	> 400	< 6	< 6(5)
T1811DA	T1811	50	.53	15 ± 9 (HAZ)(3)	> 400	10	< 32
		70	.75	15 ± 9 (HAZ)(3)	> 400	< 6	< 6(5)
T164STA	T175A	60	.50	15 ± 9 (FZ)(2)	-	< 6	< 6(5)
		80	.68	15 ± 9 (FZ)(2)	> 400	< 6	< 6(5)
T164STA	T164	60	.50	> 24	-	< 6	< 6(5)
		80	.68	Between 175 & 384(FZ,HAZ)(4)	> 600	< 6	< 6(5)

NOTES: (1) Test stress divided by parent-material yield strength at test temp.
(2) Stress-corrosion cracking in fusion zone only.
(3) Stress-corrosion cracking in heat-affected zone only.
(4) Stress-corrosion cracking both in fusion and heat-affected zones.
(5) Values obtained by interpolation from Figures 8 - 15.

MECHANISM FOR CYCLIC STRESS-CORROSION BEHAVIOR

The cyclic stress-corrosion data obtained on this program indicate that under the test conditions employed, cyclic exposures alleviated hot-salt stress-corrosion cracking but did not eliminate the problem. These data do not fully explain the absence of hot-salt stress corrosion in titanium parts operating in aircraft at elevated temperatures in a marine atmosphere. At the inception of the program, an hypothesis was formulated to explain this based on the following assumptions:

a. A chemical cell is necessary for stress-corrosion cracking of titanium alloys.

b. A nucleation time at elevated temperature is necessary to establish this cell.

c. Cooling the material changes the chemical cell in some manner.

d. Upon reheating, time is required to renucleate the stress-corrosion chemical cell before cracking is possible.

If typical flight profiles involve thermal exposure times less than the nucleation time, stress-corrosion cracking should not occur.

Species of the type $TiCl_x$ (primarily $TiCl_2$) form during hot-salt stress corrosion,[7,8] and such compounds would be expected to decompose in air at ambient conditions. Thus, a chemical cell involving $TiCl_2$ might fulfill the assumptions of the above hypothesis.

Rideout[9] suggested that hydrogen is responsible for hot-salt stress-corrosion cracking. Hydrogen could evolve from a reaction between $TiCl_2$ and moisture as follows: $TiCl_2 + H_2O \rightarrow TiOCl_2 + 2H$, and we have confirmed the presence of $TiOCl_2$ by X-ray diffraction measurements.

It is not now clear whether the reaction of sodium chloride and titanium to form $TiCl_2$ or the reaction of $TiCl_2$ and moisture to form nascent hydrogen is responsible for stress-corrosion cracking. In either case, the reaction kinetics of $TiCl_2$ should provide insight into the kinetics for formation of the chemical cell responsible for stress corrosion.

Accordingly, X-ray diffraction tests were conducted on unstressed, sheet alloys to determine the time to form $TiCl_2$ at elevated temperature and the time to decompose the compound at room temperature. These alloys were coated with 0.001 inch of NaCl. The standard 0.002 inch coating could not be utilized because the diffracted X-ray beams were absorbed by the thicker salt-layer. The specimens were heated to test temperature in two hours and held 8-12 hours beyond the time required to detect $TiCl_2$. Cooling to room temperature required approximately 35 minutes.

The results shown below are semi-quantitative because approximately 3% of crystalline $TiCl_2$ had to be present before it could be detected.

ALLOY	TEMP.	INITIAL HEATING CYCLE: TIME TO FORM $TiCl_2$	INITIAL HEATING CYCLE: TIME TO DECOMPOSE $TiCl_2$ AT ROOM TEMP.	RE-HEATING CYCLE: TIME TO FORM $TiCl_2$
Ti811DA	730F	4.5 hrs.(1)	Between 2 & 48 hrs.	-----
Ti811DA	650F	0.5 hrs.	4.5	5 hrs.
Ti811DA	550F	4.5 hrs.	4.0	-----
Ti64STA	650F	16,17 hrs.	4.5	
B120A	650F	0.25 hrs.	5.0	-----

(1) After 6.5 hours at temperature, $TiCl_3$ was also detected.

The formation time for $TiCl_2$ on Ti811DA sheet followed a "C" curve relationship with respect to temperature with the minimum formation time near 650F. Results for the Ti64STA and B120A sheet alloys indicated that the formation time for $TiCl_2$ was also dependent upon substrate composition or structure. However, the time required to decompose the $TiCl_2$ at room temperature was essentially constant for all three alloys and appeared to be controlled by diffusion of moisture or oxygen through the layer of salt plus corrosion product.

At 650F, $TiCl_2$ formed very rapidly on Ti811DA during the initial heating cycle. Upon reheating the sample, the time to reform a much smaller amount of $TiCl_2$ increased from 0.5 hours to 5 hours. This effect was presumably caused by the partial depletion of NaCl in intimate contact with active sites on the titanium. Thus, formation of $TiCl_2$ probably required diffusion of NaCl and Ti across the corrosion-product interface formed during the initial heating cycle. The rate for this process would be slower than the rate of formation of $TiCl_2$ during the initial cycle when NaCl and Ti were in intimate contact.

At 650F, $TiCl_2$ formed very rapidly on Ti811DA and B120A and very slowly on Ti64STA compared to the 3-hour hold time at temperature which was employed for the cyclic-stress-corrosion tests. The time required to form $TiCl_2$ on Ti811DA at 550F was approximately 50 percent longer than the hold time employed for the cyclic tests. In addition, the time required to decompose $TiCl_2$ on all three alloys was longer than the cooling time employed for the 550F and 650F cyclic-stress-corrosion tests.

It must be appreciated that the nucleation times reported for stress-corrosion cracking actually represented the time required to develop the necessary chemical cell plus the time for the chemical cell and stress to produce a crack in a given titanium alloy. Nevertheless, at high stresses the time required for the chemical cell and stress to produce cracking was apparently quite short at 550F and 650F, as evidenced by the short stress-corrosion nucleation times observed.

These results indicate that both the time at elevated temperature and the time at room temperature are critical factors in cyclic hot-salt stress corrosion. This suggests two reasons why the cyclic thermal exposures used for this program did not eliminate stress corrosion. First, the hold times at elevated temperature were sufficiently long to permit formation of $TiCl_2$ and its interaction with the applied stress to initiate stress corrosion cracks in some cases. Secondly, the hold time at room temperature was much less than the time required to decompose $TiCl_2$. As a result, even alloys which required more than 3 hours at temperature to form detectable amounts of $TiCl_2$ would eventually form the compound because the hold times at room temperature were not sufficient to decompose it between successive heatings.

SPECIAL CYCLIC TESTS

To investigate this concept further, several stress corrosion tests were conducted on smooth tensile specimens of Ti811DA sheet at 550F using the special cycle described below (Figure 5):

1. Heating to 550F in 10 minutes.
2. Holding at temperature for one hour and 45 minutes.
3. Cooling to room temperature in 55 minutes.
4. Holding at room temperature for 5 hours and 10 minutes.

The time at temperature was approximately one-half the time required to detect by X-ray diffraction, the formation of $TiCl_2$ at 550F in this alloy. The time at room temperature was approximately 30 percent longer than the time required to decompose $TiCl_2$ within the limits of detectability by X-ray diffraction.

Specimens were tested using a 0.001 inch NaCl coating to provide direct correlation with the X-ray diffraction data and a 0.002 inch NaCl coating for correlation with the standard cyclic results. Results are shown in Table XI, along with comparative data obtained using the standard cycle. The specimens exposed to the modified cycle showed no cracking after total times-at-temperature well beyond the cyclic nucleation times obtained using the standard cycle.

These limited results are highly encouraging because they suggest that hot-salt stress corrosion may be eliminated, even at high stresses, by controlled thermal cycles. These cycles must be controlled to the extent that the time at temperature is less than the time to form $TiCl_2$, or if some $TiCl_2$ forms, the hold time at room temperature must be greater than the time required to decompose $TiCl_2$, based upon X-ray diffraction measurements.

Whether these allowable cycles are practical in terms of a Mach 3 mission will depend upon the reaction kinetics of $TiCl_2$ for the specific alloy. Additional effort is needed to establish these reaction kinetics for various alloys by X-ray diffraction measurements and to further confirm this hypothesis by additional cyclic stress-corrosion tests.

TABLE XI

CYCLIC NUCLEATION TIMES OF Ti-8Al-1Mo-1V(DA)

SHEET AT 550F - SPECIAL CYCLE

NaCl COATING THICKNESS (inch)	TEST STRESS (ksi)	CYCLIC NUCLEATION TIME - SPECIAL CYCLE(1) (hours)	CYCLIC NUCLEATION TIME - STANDARD CYCLE(2) (hours)
0.002	80	>102	43 ± 8
0.001	80	>144	-
0.002	70	>168	54 ± 18
0.001	70	>168	-

NOTES: (1) Special Cycle:

1. Heating to 550F in 10 minutes.
2. Holding at 550F for one hour and 45 minutes.
3. Cooling to room temperature in 55 minutes.
4. Holding at room temperature for 5 hours and 10 minutes.

(2) Standard Cycle:

1. Heating to 550F in 10 minutes.
2. Holding at 550F for 3 hours.
3. Cooling for 50 minutes.

V CONCLUSIONS

1. Hot-salt stress corrosion of fatigue-cracked titanium alloys is not controlled by fracture mechanics because new surface cracks nucleated and grew in preference to an existing fatigue crack.

2. Of the alloys studied, only Ti811MA was susceptible to hot-salt stress corrosion at 450F.

3. Nucleation times for hot-salt stress corrosion were highly stress-dependent under continuous thermal exposures and under the specified, cyclic, thermal exposure used in this program. Threshold stress-levels below which stress corrosion did not occur were essentially equal under continuous and cyclic exposures.

4. At high stresses, well above threshold levels, continuous and cyclic stress-corrosion nucleation times were essentially equivalent in most of the alloys.

5. At high stress levels, continuous and cyclic nucleation times at 650F were less than a single Mach 3 mission for many alloys. At 550F, continuous and cyclic nucleation times were generally greater than a single Mach 3 mission, but several orders of magnitude less than the overall design life of a Mach 3 aircraft.

6. Welding produced no detrimental effects on the stress corrosion behavior of weldments. Continuous and cyclic stress-corrosion nucleation times at 550F for welded specimens of Ti811DA and Ti64STA were substantially longer than those observed on the parent materials. At 650F, continuous nucleation times for welded specimens were equal to or slightly longer than continuous nucleation times for the parent materials, but cyclic nucleation times were substantially longer. The behavior of welded specimens may have been influenced by the presence of compressive surface residual stresses produced during specimen preparation.

7. There is an excellent possibility for eliminating hot-salt stress corrosion even at high stresses if the thermal cycles to which the material is exposed can be controlled. The time at temperature should be less than the time to form $TiCl_2$, and the time between cycles at room temperature, greater than the time required to decompose $TiCl_2$. X-ray diffraction techniques may be used to determine the kinetics of the reaction in which $TiCl_2$ is formed.

REFERENCES

1. G. J. Heimerl, D. N. Braski, D. M. Royster, and H. L. Dexter, "Salt Stress Corrosion of Ti-8Al-1Mo-1V Alloy Sheet at Elevated Temperatures," Paper No. 42, presented at Fifth Pacific Area National Meeting of ASTM, Seattle, Washington, Oct.-Nov. 1965.

2. G. E. Dieter, Jr., "Mechanical Metallurgy," McGraw-Hill Book Company, Inc., New York, N. Y. 1961.

3. D. N. Braski and G. J. Heimerl, "The Relative Susceptibility of Four Commercial Titanium Alloys to Salt Stress Corrosion at 550F," NASA Technical Note D-2011, Langley Research Center, Langley Station, Hampton, Virginia, 1963.

4. A. Phillips, V. Kerlins, B. V. Whiteson, Electron Fractography Handbook, ML-TDR-64-416, January 1965, AF33(657)-11127, Douglas Aircraft Company, Santa Monica, California.

5. R. V. Turley and C. H. Avery, "Elevated-Temperature Static and Dynamic Sea-Salt Stress Cracking of Titanium Alloys," from "Stress-Corrosion Cracking of Titanium," ASTM STP 397, 1966, pp 1-30.

6. R. Newcomer, H. C. Tourkakis, and H. C. Turner, "Elevated Temperature Stress Corrosion Resistance of Titanium Alloys," Corrosion, Vol. 21, No. 10, October 1965, pp 307-315.

7. F. A. Crossley, C. J. Reichel, and C. R. Simcoe, "The Determination of the Effects of Elevated Temperatures on the Stress Corrosion Behavior of Structural Materials," WADD Technical Report 60-191, May 1960.

8. D. N. Braski, "Preliminary Investigation of Effect of Environmental Factors in Salt Stress Corrosion Cracking of Ti-8Al-1Mo-1V at Elevated Temperatures," NASA TMX-1048, December 1964.

9. S. P. Rideout, "The Initiation of Hot-Salt Stress Corrosion Cracking of Titanium Alloys," presented at ASTM Symposium on Applications Related Phenomena in Titanium Alloys, 18-19 April 1967, Los Angeles, California.

Unclassified
Security Classification

DOCUMENT CONTROL DATA - R&D

(Security classification of title, body of abstract and indexing annotation must be entered when the overall report is classified)

1. ORIGINATING ACTIVITY (Corporate author)	2a. REPORT SECURITY CLASSIFICATION
Northrop Norair Division of Northrop Corporation Hawthorne, Calif. 90250	2b GROUP

3. REPORT TITLE

Cyclic Hot Salt Stress Corrosion of Titanium Alloys

4. DESCRIPTIVE NOTES (Type of report and inclusive dates)

Summary of investigation extending from 1 March 1966 to 30 May 1967.

5. AUTHOR(S) (Last name, first name, initial)

L. H. Stone
A. H. Freedman

6. REPORT DATE	7a. TOTAL NO. OF PAGES	7b. NO. OF REFS
September 1967	47	9

8a. CONTRACT OR GRANT NO.	9a. ORIGINATOR'S REPORT NUMBER(S)
AF 33(615)-3642 b. PROJECT NO. 7381	NOR 67-151
c.	9b. OTHER REPORT NO(S) (Any other numbers that may be assigned this report)
d.	AFML-TR-67-289

10. AVAILABILITY/LIMITATION NOTICES This document is subject to special export controls and each transmittal to foreign governments or foreign nationals may be made only with prior approval of the Air Force Materials Laboratory (MAAS), Wright-Patterson Air Force Base, Ohio 45433.

11. SUPPLEMENTARY NOTES	12. SPONSORING MILITARY ACTIVITY
	Air Force Materials Laboratory Research & Technology Division Wright-Patterson AFB, Ohio 45433

13. ABSTRACT Hot-salt stress-corrosion cracking of Ti-6Al-4V, Ti-8Al-1Mo-1V, Ti-13V-11Cr-3Al, Ti-6Al-6V-2Sn, and Ti-679 was investigated for both continuous exposure and a specified, cyclic, thermal exposure representing a typical Mach 3 mission. The effects of heat treatment and material thickness were also studied.

Initial tests of fatigue-cracked specimens showed that hot-salt stress-corrosion cracking is not controlled by fracture mechanics because new surface cracks nucleate and grow in preference to an existing fatigue crack. Therefore, all subsequent tests were conducted on smooth specimens.

At 450F, only mill-annealed Ti-8Al-1Mo-1V showed stress-corrosion cracking. At 550 and 650F, individual threshold values of stress were established for each material below which no cracking occurred for either continuous or cyclic exposure. Most of these threshold levels lay between 0.35 and 0.50 of the yield strength at 550F and between 0.25 and 0.45 of the yield strength at 650F.

At stress levels just above threshold values, cyclic nucleation times were substantially longer than continuous nucleation times. As the stress level increased, this difference decreased, and at high stress levels, both nucleation times were essentially the same. Welding produced no detrimental effects on the stress corrosion behavior of Ti-8Al-1Mo-1V and Ti-6Al-4V. Welded specimens had much longer nucleation times, cyclic or continuous, than the parent metal at 550F; at 650F, the continuous nucleation times for welded specimens approximated those for the parent materials, but the cyclic nucleation times were substantially longer. The behavior of welded specimens may have been influenced by the presence of compressive

DD FORM 1 JAN 64 1473

Unclassified
Security Classification

surface residual stresses produced during specimen preparation.

The kinetics of the formation of $TiCl_2$ on NaCl-coated titanium alloys and of its decomposition at room temperature were measured by X-ray diffraction. Detectable amounts of $TiCl_2$ appeared after periods of 0.25 to 17 hours for various alloys at temperatures from 550 to 730F. Decomposition times at room temperature were relatively constant at 4 to 5 hours. Specimens were subjected to a special cycle of heating at 550F for less time than that to produce detectable $TiCl_2$ and holding at room temperature for longer than needed to decompose $TiCl_2$. These specimens did not show cracking in times well beyond the nucleation times for the standard cycle.

The results of this program indicate a strong possibility for eliminating hot-salt stress corrosion of titanium structures operating above 550F, even at high stresses, if the thermal cycles to which the structure is exposed can be controlled. The time at temperature should be less than the time to form $TiCl_2$, and the time between cycles at room temperature greater than the time required to decompose $TiCl_2$.

This abstract is subject to special export controls and each transmittal to foreign governments or foreign nationals may be made only with prior approval of Air Force Materials Laboratory (MAAS) Wright-Patterson Air Force Base, Ohio 45433.